HHS Public Access

Author manuscript

DNA Repair (Amst). Author manuscript; available in PMC 2017 June 01.

Published in final edited form as:

DNA Repair (Amst). 2016 June ; 42: 11–25. doi:10.1016/j.dnarep.2016.04.001.

SUMOylation of Rad52-Rad59 synergistically change the outcome of mitotic recombination

Sonia Silva[a,1,2], **Veronika Altmannova**[b,1], **Nadine Eckert-Boulet**[a], **Peter Kolesar**[b], **Irene Gallina**[a], **Lisa Hang**[c], **Inn Chung**[c], **Milica Arneric**[c], **Xiaolan Zhao**[c], **Line Due Buron**[d], **Uffe H. Mortensen**[d], **Lumir Krejci**[b,e,f], and **Michael Lisby**[a,*]

[a]Department of Biology, University of Copenhagen, Ole Maaløes Vej 5, DK-2200 Copenhagen N, Denmark

[b]Department of Biology, Masaryk University, Kamenice 5/A7, 62500 Brno, Czech Republic

[c]Molecular Biology Program, Memorial Sloan-Kettering Cancer Center, New York, NY 10065, USA

[d]Department of Systems Biology, Technical University of Denmark, Building 223, 2800 Kgs. Lyngby, Denmark

[e]National Centre for Biomolecular Research, Masaryk University, Kamenice 5/A4, Brno 625 00, Czech Republic

[f]International Clinical Research Center, Center for Biomolecular and Cellular Engineering, St. Anne's University Hospital Brno, Brno, Czech Republic

Abstract

Homologous recombination (HR) is essential for maintenance of genome stability through double-strand break (DSB) repair, but at the same time HR can lead to loss of heterozygosity and uncontrolled recombination can be genotoxic. The post-translational modification by SUMO (small ubiquitin-like modifier) has been shown to modulate recombination, but the exact mechanism of this regulation remains unclear. Here we show that SUMOylation stabilizes the interaction between the recombination mediator Rad52 and its paralogue Rad59 in *Saccharomyces cerevisiae*. Although Rad59 SUMOylation is not required for survival after genotoxic stress, it affects the outcome of recombination to promote conservative DNA repair. In some genetic assays, Rad52 and Rad59 SUMOylation act synergistically. Collectively, our data indicate that the described SUMO modifications affect the balance between conservative and non-conservative mechanisms of HR.

Keywords

Homologous recombination; Rad52; Rad59; Srs2; Rad51; SUMOylation

[*]Corresponding author. mlisby@bio.ku.dk (M. Lisby).

[1]These authors contributed equally to this work.

[2]Current address: Centro Andaluz de Biología Molecular y Medicina Regenerativa CABIMER, Universidad de Sevilla, Seville, Spain.

Conflict of interest

The authors declare that there are no conflicts of interest.

1. Introduction

DNA double-strand breaks (DSBs) are one of the most deleterious types of DNA lesions. If not faithfully repaired, a single break can lead to translocations and genome instability or if not repaired to aneuploidy or cell death. In budding yeast, homologous recombination (HR) is the preferred pathway for repairing DSBs, which is mediated by the proteins encoded by the *RAD52* epistasis group. This Rad52-mediated repair pathway can be divided into two sub-pathways, depending on whether repair is *RAD51*-dependent or -independent [1]. Notably, non-conservative *RAD51*-independent HR via single-strand annealing (SSA) relies on the *RAD52* paralogue *RAD59* [2,3], and on *RAD52* itself [4–8]. Similarly, break-induced replication, alternative lengthening of telomeres and inverted-repeat recombination can also proceed by either the Rad51 or Rad59 pathways [9–11], but the control of pathway choice is not fully understood. Most DSBs in mitotic cells are repaired by *RAD51*-dependent recombination, by which a Rad51 filament covers the 3′ single-stranded DNA (ssDNA) tails generated by resection of the break and initiates strand invasion at an intact homologous sequence, yielding a gene conversion (GC) event [12,13]. Rad52 forms a heptameric ring that acts as a mediator for displacing replication protein A (RPA) and for loading Rad51 onto ssDNA to form the Rad51 nucleoprotein filament [14]. Rad59 is homologous to the N-terminal portion of Rad52, comprising the DNA-binding and multimerization domains [9]. Since Rad59 is able to interact directly with Rad52, it has previously been suggested that Rad52 and Rad59 might form heteromeric rings [15,16]. In addition, Rad59 exhibits ssDNA annealing activity but does not interact directly with RPA or Rad51 [17–21].

During homologous recombination, Rad51 presynaptic filament formation is counteracted by the action of Srs2, which displaces Rad51 from ssDNA through its ATP-dependent translocase activity [22–26]. Null mutants of *srs2* display increased cell death when exposed to DNA damaging agents, either as a result of accumulation of toxic recombination intermediates [27–29] or due to an inability to recover from checkpoint arrest [30,31]. Increased cell death of *srs2*Δ cells is accompanied by a hyperrecombination phenotype for both intrachromosomal and sister-chromatid gene conversion [23]. Finally, Rad52 and Rad59 are also important for catalyzing spontaneous recombination events [9,32], which can be initiated by DSBs [33] or at single-stranded gaps and other non-DSB lesions [34–36].

Post-translational modifications play a critical role in genome maintenance. One such modification is SUMOylation, the reversible covalent attachment of a small ubiquitin-like modifier (SUMO/Smt3) onto one or several lysines on a target protein [37–41]. A number of HR factors are targeted by SUMOylation upon DNA damage [42,43]. Together with Rad52 and Rad59 [44,45], the RPA complex [45], the Mre11-Rad50-Xrs2 complex (MRX) [42], and Srs2 are also SUMOylated [46,47]. The relevance of these SUMO modifications in regulating HR remains mostly unclear, but in some instances it has been possible to demonstrate a direct role of SUMOylation in regulating protein–protein interactions, protein localization or activity [41]. In particular, SUMOylation of Rad52 at lysines 43, 44 and 253 (using the original amino acid numbering [48] or lysines 10, 11 and 220 when considering the first actual start codon [49]) is induced by DNA damage and shields the protein from proteasomal degradation [44], inhibits its DNA binding and strand annealing activities [50],

and inhibits Rad52-mediated recombination within the nucleolus [51]. Important for our understanding of these effects, SUMOylated proteins can be recognized and bound non-covalently by other proteins through a SUMO-interacting motif (SIM) as reported for Srs2 and SUMOylated PCNA, and for Rad51 and SUMOylated Rad52 [46,52–54].

In this study we examined the effects of SUMOylation on Rad52 and Rad59 activities during HR. Using a combination of genetic, biochemical and cell biological approaches we present evidence that SUMOylation stabilizes the Rad52-Rad59 complex in an active conformation and synergistically regulate the balance between conservative and non-conservative mechanisms of HR.

2. Materials and methods

2.1. Yeast media, strains and constructs

Yeast extract-peptone-dextrose (YPD) medium, synthetic complete (SC) medium, synthetic complete supplemented with an additional 100 μg/ml adenine (SC + Ade) or lacking X (SC-X), and 5′-fluoro-orotic acid (5-FOA) medium were prepared as described previously in Ref. [55]. SC medium supplemented with 2% raffinose was prepared like SC medium with glucose, substituting glucose with raffinose. Strains used in this study are shown in Table S1. Plasmids used in this study are shown in Table S2. Primers with corresponding sequences used in this study are listed in Table S3. All mutant strains for *RAD52* and *RAD59* were generated by gene targeting essentially as described elsewhere [56]. The presence of the *rad52-F110A* mutation was analyzed by colony PCR and digestion with *HaeII* restriction enzyme. Rad52 C-terminal tagging with *SMT3ΔGG* was done using primers RAD52fw2244, RAD52-SMT3-R, RAD52-SMT3ΔGG-F, RAD52down SMT3-A-F and SMT3ΔGG-R to generate strain SS55. CFP was added to the C-terminus of the *rad52-SMT3ΔGG* allele using primers SMT3F, SMT3ΔGG-YFP-Rv, RAD52-Tdown and RAD52-down to generate strain SS184. Rad59 C-terminal tagging with *SMT3ΔGG* was done using primers RAD59Fw, RAD59-SMT3-Rv, RAD59-SMT3ΔGG-Fw2, RAD59-termRv, SMT3-A-F and SMT3ΔGG-Rv to generate strain SS43. In order to obtain isogenic VC-tagged *RAD52* strains, a PCR product containing *VC155-T_{ADH1}-kanMX6* was amplified from genomic DNA of the strain ML659-1B harbouring *RAD52-VC155-T_{ADH1}-KanMX6*. To generate *RAD52-VC*, *rad52-3KR-VC* and *rad52-F110A-VC*, the primer pair RAD52fwd2244 and RAD52-down was used to generate the VC fragments harbouring complementary overhangs to target integration of the construct at the C-terminal end of the endogenous locus for *RAD52* in the target strains ML8-9A, NEB142-7C, and SS87-1D, respectively, and in that order generating strains ML744, ML745 and ML748. For creating *rad52-SMT3ΔGG-VC*, primers SMT3ΔGG-F2 and RAD52-down were used to generate the VC fragment that was integrated into SS55 to generate strain ML746. To obtain VN-tagged *RAD59* strains in W303 background, a PCR product containing *VN173-T_{ADH1}-Kl.URA3* was amplified from genomic DNA of the strain from the VN library strain (Bioneer) harbouring *RAD59-VN173-T_{ADH1}-Kl.URA3*. To generate *RAD59-VN*, the primer pair RAD59fwd2385 and RAD59down.rv was used and the generated fragment integrated into strain W4700-10C to create ML743. To generate *rad59-2KR-VN*, the primer pair RAD59K-Cterm.fw and RAD59down.rv was used and the generated fragment integrated into strain

ML386-2C to create ML742. For creating *rad59-SMT3ΔGG-VN*, SMT3ΔGG-F2 and RAD59down.rv were used to generate the VN fragment that was integrated into SS43 to generate strain ML747. The sequence integrity of all strains generated using fragment integration was confirmed by sequencing. The above-mentioned strains were crossed to yield strains carrying combinations of VC and VN-tagged Rad52 and Rad59 variants. For testing DNA damage sensitivity, cells were grown over-night at 30 °C to saturation in liquid YPD media and 10-fold serial dilutions were prepared for spotting. DNA damage sensitivity was assayed by allowing cells to grow for up to 72 h at 30 °C after spotting onto solid YPD or YPD containing Zeocin (Invitrogen) or methyl methanesulfonate (MMS) (Sigma) to the final concentrations stated in the figure legends.

2.2. Microscopy

Cells were grown shaking in liquid SC + Ade medium at 25 °C unless stated otherwise, to OD_{600} (optical density) = 0.2–0.3, collected by centrifugation at 2000 *g* and processed for fluorescence microscopy as described previously in Ref. [57]. For this study, the following fluorophores were used: cyan fluorescent protein (CFP, clone W7) [58], yellow fluorescent protein (YFP, clone 10C) [59] and red fluorescent protein (RFP, clone yEmRFP) [60]. Fluorophores were visualized on an AxioImager Z1 (Carl Zeiss MicroImaging, Inc.) equipped with a 100× objective lens (Zeiss PLAN-APO, NA 1.4), a cooled Orca-ER CCD camera (Hamamatsu, Japan), differential interference contrast (DIC), and a Zeiss HXP120C illumination source, or on a Deltavision Elite microscope (Applied Precision, Inc.) equipped with a 100× objective lens (Olympus U-PLAN S-APO, NA 1.4), a cooled Evolve 512 EMCCD camera (Photometrics, Japan), and an Insight solid state illumination source (Applied Precision, Inc.). Images were acquired using Volocity (PerkinElmer) or softWoRx (Applied Precision, Inc.) software. Image analysis and fluorescence intensity quantification were done using Volocity software (PerkinElmer). Images were pseudo-coloured according to the approximate emission wavelength of the fluorophores.

2.3. Detection of Rad59 in vivo SUMOylation

Detection of Rad59 SUMOylation was described in Ref. [45]. In brief, the TAP tagged Rad59 strains were treated with 0.3% MMS for 2 h before harvest. Cell pellets were broken by glass bead beating in the presence of TCA. Subsequently, the protein pellets were resuspended, Rad59-TAP protein was immunoprecipitated by IgG beads and analyzed by western blotting. The antibodies used were anti-SUMO [61] and anti-ProA (Sigma). Alternatively, whole cell extracts were analyzed for the presence of SUMOylated Rad59-TAP protein by using the anti-ProA antibody.

2.4. DNA substrates

Oligonucleotides were purchased from VBC Biotech and TAG Copenhagen A/S. The sequences of oligonucleotides are shown in Supplementary Table 3. Oligo-1 and Oligo-3 were modified with fluorescein at the 5′ end.

2.5. Recombinant protein expression and purification

2.5.1. Purification of His-tagged Rad59—The various Rad59 species were expressed and purified as described in Ref. [18] with small modifications. Briefly, the *Escherichia coli* strain BL21(DE3)pLysS transformed with plasmid for expression of Rad59 protein was induced with 0.4 mM IPTG for 20 h at 18 °C. The cells were pelleted and stored at −80 °C. The cell pellet (11 g) was resuspended in 40 ml of cell breakage buffer (20 mM Tris, pH 8.0, 10% glycerol) containing 300 mM NaCl, 7 mM β-mercaptoethanol, 0.1% Triton X, and protease inhibitor cocktail (pepstatin, leupeptin). Cells were lysed by two thaw/freeze cycles and shortly sonicated. The crude extract was clarified by centrifugation (100,000 *g*, 1 h, 4 °C). The supernatant was mixed with 800 μl of His-Select Nickel Affinity Gel (Sigma) washed in cell breakage buffer (CBB) (50 mM Tris–HCl, pH 7.5, 10% sucrose, 2 mM EDTA) containing 300 mM NaCl for 1 h at 4 °C. The beads were washed with 10 ml CBB buffer containing 300 mM NaCl and 5 mM imidazole. Rad59 was then eluted in steps with CBB buffer containing 300 mM NaCl and 150/300/500/1000/2000 mM imidazole. The fractions eluted from nickel column from 500 to 2000 mM imidazole were concentrated in Amicon concentrator (10,000 MWCO) to 3 μg/l and stored in small aliquots at −80 °C.

2.5.2. Purification of Siz1 and Siz2—The plasmids (a kind gift from Y. Kikuchi) expressing Siz1 (1–465) and Siz2 proteins containing $(His)_6$-affinity tag were introduced into *E. coli* strain BL21(DE3). Overnight cultures grown in 2xTY medium were diluted 100-fold into fresh 2xTY medium and incubated at 37 °C. The overexpression of Siz1 and Siz2 was induced by adding 0.1 mM IPTG followed by an incubation at 16 °C overnight. The cells were harvested by centrifugation and stored at −80 °C. Extracts from 10 g of cell paste were prepared by sonication in 30 ml of CBB buffer containing 150 mM KCl, 0.01% NP40, 1 mM β-mercaptoethanol and protease inhibitor cocktail. The lysates were clarified by ultracentrifugation. The resulting supernatants were incubated with 700 μl His-Select Nickel Affinity Gel (Sigma) for 1 h at 4 °C. The bead-bound proteins were washed with 7 ml of buffer K (20 mM K_2HPO_4, pH 7.4, 10% glycerol, 1 mM EDTA, 0.01% NP40, and 1 mM β-mercaptoethanol) containing 50 mM KCl followed by 7 ml of buffer K containing 50 mM KCl and 10 mM imidazole. The bound proteins were eluted with buffer K containing 50 mM KCl and 150, 300, 500, or 1000 mM imidazole. The fractions containing Siz1 or Siz2 protein were pooled, loaded onto a 1 ml Heparin column and then eluted using a 10 ml gradient of 100–1000 mM KCl in buffer K. The peak fractions were concentrated in a Vivaspin (30,000 MWCO) to 3 μg/l and stored at −80 °C.

2.5.3. Purification of other proteins—MBP-Rad59, RPA, His-Rad52 and SUMO machinery proteins (GST-Aos1/Uba2, His-Ubc9, His-Flag-Smt3) were expressed and purified as described previously in Refs. [50,62–64].

2.6. In vitro *SUMOylation assay*

The assay was performed as described, with some modifications [50]. Purified Aos1/Uba2 (400 nM), Ubc9 (2.8 μM), Smt3 (5.6 μM), 2.5 mM ATP, buffer S (50 mM HEPES, 10 $MgCl_2$, 0.1 mM DTT) and 5.6 μM of various Rad59 proteins were mixed in a 10 μl reaction volume and incubated at 4 °C for 1 h. In the indicated cases, 50 nM Siz1 or 50 nM Siz2

were added to the mixture. Reactions were stopped by addition of 10 μl of SDS Laemmli buffer and analyzed by SDS-PAGE and western blotting.

2.7. Electrophoretic mobility shift assay

The fluorescently labelled DNA substrate (Oligo-5, 0.3 μM nucleotides) was incubated with indicated amounts of various forms of Rad59 protein at 37 °C in 10 μl of buffer D (40 mM Tris–HCl, pH 7.5, 50 mM KCl, 1 mM DTT and 100 μg/ml bovine serum albumin (BSA)). Following the addition of gel loading buffer (60% glycerol, 10 mM Tris–HCl, pH 7.4 and 60 mM EDTA), the reaction mixtures were resolved in 13% native polyacrylamide gels in TBE buffer (40 mM Tris–HCl, 20 mM boric acid, 2 mM EDTA, pH 7.5) at 4 °C, and the DNA species were analyzed using Multi Gauge software (Fuji).

2.8. Single-strand annealing assay

The assay was performed essentially as described in Ref. [50]. The fluorescently labelled Oligo-1 and unmodified Oligo-2 (0.25 μM nucleotides) were incubated separately at 37 °C for 3 min in the absence or presence of RPA (20 nM) in 12.5 μl of buffer D. Increasing amounts of various forms of Rad59 were added to the reaction mixtures containing Oligo-2 and then mixed with Oligo-1. After 8 min incubation at 37 °C, 9 μl of the reaction mixture was removed and treated with 0.5% SDS, and 500 μg/ml proteinase K for 10 min at 37 °C. The annealing reactions were resolved in 10% native polyacrylamide gels run in TBE buffer. The efficiency of DNA annealing was quantified as the percentage of the fluorescently labelled Oligo-1 that had been converted into the double-stranded form.

2.9. Affinity pull-down assay

MBP-tagged Rad59 or Smt3-Rad59 (2.33 μM) were mixed with Rad52 (2.9 μM) in 25 μl buffer K containing 50 mM KCl and incubated for 15 min at 10 °C followed by adding 25 μl of amylose beads. After 30 min incubation, the beads were washed and treated with SDS-Laemmli buffer to elute bound proteins. The supernatant containing unbound Rad52 and the SDS eluate (7.5 μl each) were analyzed on 7.5% SDS-PAGE stained with Coomassie Brilliant Blue.

2.10. Yeast two-hybrid analysis

The yeast two-hybrid analysis was carried out with plasmids pGAD-*RAD52* (pSLH217) [65], pGBD-*RAD52* (pSLH127) [65], pGAD-*RAD59* [18], and pGBD-*RAD51* [66]. The *rad52-K43,44,253R* mutation was introduced both in pSLH217 and pSLH127 by two successive rounds of site-directed mutagenesis using the primers pR55 and pR56 for K43,44 and primers pR995 and pR996 for K253, generating pPKS01 and pPKS06. The *rad52-F110A* mutation was introduced into pSLH217 and pSLH127 by site-directed mutagenesis using primers RAD52F110-Fw and RAD52F110A-Rv generating plasmids pPKS02 and pPKS07. The *rad59-K207,228R* mutation was introduced into plasmids pGAD-RAD59 and pGBD-RAD59 by two successive rounds of site-directed mutagenesis using primers pR107 and pR108 for K207 and pR641 and pR642 for K228, generating pPKS04 and pPKS09. All primers are described in Supplementary Table 3. For testing SUMO interactions pGAD-*UBC9* [67], pGAD-*SMT3* (pF11) and pGAD-*SMT3ΔGG* (pF12) (S. Åström, unpublished)

were used. For assaying SUMO interactions with Rad52, *MAT***a** and *MATα* derivatives of PJ69-4A were used as reporter strains [68]. For testing Rad52 self-association and interaction with the different Rad59 mutant variants, the analysis was carried out in reporter strains with no endogenous *RAD52* and *RAD59* (W2274-9B and W2274-1C). The expression of the *lacZ* reporter gene was determined quantitatively by measuring β-galactosidase activity as previously described in Ref. [68] and calculating the corresponding Miller units [69].

2.11. Recombination assays

Heteroallelic and direct-repeat (DR) mitotic recombination was measured in diploid and haploid strains, respectively. The procedure for determining mitotic recombination rates and their standard deviation was done essentially as described before [70–74] with the following exception: all cultures were grown in liquid SC + Ade medium at 30 °C prior to plating. For direct-repeat recombination, Leu+ recombinants were replica-plated to SC-Leu-Ura after 2 days to score for loss of the *URA3* marker. *LEU2* recombination rates were based on fluctuation analysis of 9–19 trials for each genotype and calculated by the FALCOR MSS Maximum Likelihood algorithm [73,74]. Break-induced replication (BIR) and inverted-repeat recombination were analyzed essentially as described in Refs. [9,75]. In brief, the *ade2* inverted-repeat assay contains two *ade2* heteroalleles integrated at the *HIS3* locus in an inverted orientation. The *ade2* alleles are non-functional, resulting in red colonies on non-selective media. Recombination between the two alleles can produce a wild type *ADE2*, resulting in a white sector within the red colony. Thus recombination level can be quantitatively determined by measuring the frequency of Ade^+ within a population of cells. The inverted-repeat assay was analyzed in a *rad51*Δ background, which makes it particularly sensitive to loss of Rad59 function [9]. In BIR assay, a linear chromosome fragmentation vector (CFV) undergoes telomere addition at one end of the vector, and the other end invades the endogenous chromosomal locus, copying sequences from the region of homology between the vector and native chromosome to the telomere. This results in a stable artificial chromosome. The *SUP11* marker on the CFV suppresses *ade2-1* in the yeast strain, leading to white colonies, whereas cells lacking CFV form red colonies. Transformants that showed very low sectoring following nonselective growth were scored as containing stable CFs. The assays were performed as described in Refs. [9,75].

2.12. Chromatin immunoprecipitation

Cells were grown shaking for 20 h at 30 °C in yeast extract-peptone containing 2% raffinose (YPR) medium, diluted to OD_{600} = 0.3 and grown to OD_{600} = 0.5 before induction of the HO endonuclease by addition of 3% galactose. Cells were fixed by addition of 1.1 ml of 36.5% formaldehyde (SIGMA, cat.no. 252549) to 40 ml of culture and rotate for 5 min at 23 °C. Fixation was quenched by addition of 2 ml of 2.5 M glycine followed by incubation for 5 min at 23 °C. Cells were collected by centrifugation at 3000 rpm for 3 min at 4 °C and washed twice in ice-cold HBS (25 mM HEPES pH 7.5, 140 mM NaCl) and once in ice-cold ChIP lysis buffer (25 mM HEPES pH 7.5, 140 mM NaCl, 1 mM EDTA, 1% NP40, 2 mM sodium deoxycholate). The pellet was frozen at −80 °C overnight. Before cell lysis, pellets were thawed on ice and resuspended in 600 μl ChIP lysis buffer containing 1 mM PMSF and complete protease inhibitor cocktail (Roche) and supplemented with 200 μl glass beads (0.5

mm). Cells were homogenized for 45 s at 4 °C by using a FastPrep-24TM 5 G Instrument (MP Biomedicals) followed by incubation on ice for 2 min. Homogenization was repeated 3 times. Cell extract was transferred to a 1.5 ml tube by centrifugation for 1 min at 1000 rpm through a hole in the bottom of the Fast-Prep tube followed by collection of chromatin by centrifugation at 13,000 rpm for 30 min at 4 °C. The supernatant was discarded and the pellet resuspended in 500 μl ChIP lysis buffer containing protease inhibitors. Next, chromatin was fragmented by sonication (50 pulses of 10 s at #3, pause 10 s; 2 °C) followed by addition of 300 μl ChIP lysis buffer containing protease inhibitors. Cell debri was collected by centrifugation at 7000 rpm for 5 min at 4 °C and soluble chromatin fraction transferred to a new tube. Next, 10 μl of the crude chromatin was transferred to 120 μl of AT4 buffer (20 mM Tris–HCl pH 7.5, 0.1 mM EDTA) containing 1% SDS (INPUT) and placed at 65 °C overnight. The remaining chromatin was divided into three 2 ml tubes with 200 μl of crude chromatin and either no antibody, 1 μl anti-Rad51 (Abcam, ab63798), or 5 μl anti-Srs2 (Santa Cruz Biotechnology, sc–11991) (IPs). The IPs were incubated with rotation for 1 h at 4 °C followed by addition of 20 μl of Dynabeads (GE Life Sciences, 10004D) to each tube and continued incubation with rotation for 2 h at 4 °C. Next, the beads were washed in 1 ml ChIP lysis buffer and transferred to a new 2 ml tube. All subsequent washes were performed at 23 °C: 1 ml of AT1 buffer with SDS freshly added (25 mM HEPES pH 7.5, 140 mM NaCl, 1 mM EDTA, 0.03% SDS) rotate 5 min, 1 ml of AT2 buffer (25 mM HEPES pH 7.5, 1 M NaCl, 1 mM EDTA) rotate 5 min, 1 ml of AT3 buffer (20 mM Tris-HCl pH 7.5, 250 mM LiCl, 1 mM EDTA, 0.5% NP40, 10 mM sodium deoxycholate) rotate 5 min, and twice 1 ml of AT4 buffer. The immunoprecipitated chromatin was released from the beads by incubation in 155 μl of AT4 buffer with 1% SDS at 65 °C for 10 min, transferred to a new tube and incubated at 65 °C overnight to reverse the crosslinking.

To purify the immunoprecipitated DNA, the IPs were first subjected to proteolytic digest using proteinase K by addition of 20 μl of 20 mg/ml proteinase K (Fermentas) and 240 μl TE buffer (10 mM Tris–HCl pH 7.5, 1 mM EDTA) followed by incubation for 2 h at 37 °C. Next, 50 μl 5 M LiCl and 450 μl phenol/chloroform were added and vortexed for 10 min. After centrifugation for 5 min at 13,000 rpm, the water phase was transferred to a new 1.5 ml tube containing 1 ml 96% EtOH, 5 μl glycogen (Roche) and 50 μl 3 M NaOAc and precipitated at −80 °C overnight. The precipitated DNA was collected by centrifugation for 5 min at 13,000 rpm, washed twice with 1 ml 70% EtOH, dried and dissolved in 50 μl ddH_2O. Real-time PCR was performed according to manufacturer's instructions using Maxima SYBR Green/ROX qPCR Master Mix (ThermoFisher Scientific, K0221). Fold enrichment of DNA at the DSB was calculated as $2^{(C_T\,\mathrm{INPUT}-C_T\,\mathrm{IP})}/2^{(C_T\,\mathrm{INPUT}-C_T\,\mathrm{NOBA})}$ and normalized to time = 0.

2.13. Statistical analysis

For live cell microscopy experiments, the significance of the differences observed among cell populations for the number of cells carrying foci was determined using one-tailed Fisher's exact test. For testing the significance of the difference between fluorescence intensity values, non-parametric Tukey's test for multiple comparison of every mean with every other mean was used. P-values with $P < 0.05$ were considered significant. The

unpaired T-test was applied to distinguish significant changes in Leu^+Ura^+ to Leu^+Ura^- events in direct-repeat recombination.

3. Results

3.1. Rad59 is SUMOylated *in vitro* and *in vivo* on lysines 207 and 228

In response to DNA damage, cells target a broad spectrum of DNA repair and checkpoint proteins for SUMOylation [42,43], including the recombination proteins RPA, Rad52, Rad59 and Srs2 [43–45,47]. To determine the relevance of Rad59 SUMOylation during HR, we performed an *in vitro* SUMOylation assay with purified Rad59, which resulted in its robust modification (30%). Using mass spectrometry, we identified lysines 207 and 228 as being conjugated with SUMO (Fig. 1A), in accordance with previously reported results [43]. However, we did not observe the previously reported SUMO modification at lysine 238 [43] and generation of a *rad59-K207,228R* (*rad59-2KR*) double mutation resulted in complete loss of SUMOylated Rad59 both *in vitro* and *in vivo* (Fig. 1B and C). Unlike Rad52 SUMOylation, which is stimulated by ssDNA [50], we find that Rad59 SUMOylation *in vitro* is unaffected by the presence of DNA and is stimulated by both SUMO ligases Siz1 and Siz2 (Supplementary Fig. S1). *In vivo*, SUMOylation of Rad59 is stimulated by exogenous DNA damage (Fig. 1D), similarly to other DNA repair proteins [42,43].

3.2. SUMOylation does not affect the biochemical activities of Rad59 *in vitro*

Previous studies have found an inhibitory effect of SUMOylation on the DNA binding and annealing activities of Rad52 [50]. These observations prompted us to test the possible effect of SUMO modification on Rad59 activities. To avoid activity differences due to variations in the total protein amounts used in each experiment, *in vitro* SUMOylation reactions were performed using the same amounts of Rad59 in the absence (no SUMOylation) or presence (SUMOylation) of ATP. First, we tested DNA binding activity of unmodified and SUMO-modified Rad59 using an electrophoretic mobility shift assay. Despite the fact that the level of modified Rad59 protein was around 30%, we did not observe any significant difference in the DNA binding affinity for either single- or double-stranded DNA (Supplementary Fig. S2A and B and data not shown). Next, we analyzed the strand annealing activity of SUMOylated Rad59 protein. Complementary ssDNA strands were incubated with unmodified or SUMO-modified Rad59 and the annealing activity was analyzed on a native polyacrylamide gel. No difference between the annealing activity of Rad59 and SUMOylated Rad59 was detected (Supplementary Fig. S2C and D). Finally, we determined that Rad59 SUMOylation did not influence the interaction between Rad59 and Rad52 *in vitro*, since Rad59 tagged with maltose-binding peptide (MBP) could pull down Rad52 irrespective of its SUMOylation status (Supplementary Fig. S2E). In conclusion, SUMOylation of Rad59 does not directly affect its biochemical activities *in vitro*.

3.3. Survival after DNA damage is largely unaffected by Rad59 SUMOylation

To determine the importance of SUMOylation in coping with DNA damage, we monitored cell survival after exposure to methyl methanesulfonate (MMS) and Zeocin (Fig. 2 we also tested if SUMOylation of Rad52 and Rad59 play redundant or distinct functions by examining combinations of SUMO-deficient mutants of both proteins (Rad52-K43,44,253R

(Rad52-3KR) and Rad59-2KR) as well as variants designed to mimic constitutively SUMOylated Rad52 and Rad59 species (Rad52-Smt3ΔGG and Rad59-Smt3ΔGG). The latter were obtained by extending the endogenous *RAD52* and *RAD59* genes at their downstream ends with a sequence encoding Smt3ΔGG. Importantly, the Smt3ΔGG moiety does not contain the last two glycines of Smt3, thereby preventing conjugation of the resulting fusion proteins to other proteins via the SUMOylation pathway [76]. The protein levels of the non-SUMOylatable and SUMO-mimetic variants of Rad52 and Rad59 were estimated from nuclear fluorescence levels of fluorescently tagged proteins (Fig. 2B and C). Consistent with a previous report [44], the non-SUMOylatable Rad52-3KR and Rad59-2KR displayed reduced protein levels, while fusion to Rad59 increased its steady-state level, suggesting that SUMOylation may shield Rad52 and Rad59 against degradation. To investigate whether SUMOylation of Rad59 acts redundantly with Srs2 to prevent or revert toxic recombination intermediates [34,77,78], we studied cell survival in both *SRS2* and *srs2*Δ backgrounds. Finally, we compared the DNA damage sensitivity of haploid and diploid cells to test whether the presence of a homologous chromosome would impact on survival of the *rad59* mutants.

The *rad59-2KR* allele alone or in combination with mutants of *SRS2* or *RAD52* does not confer additional DNA damage sensitivity (Fig. 2A and Ref. [43]). In comparison, *rad59*Δ cells are very sensitive to MMS and to a lesser extent to Zeocin at concentrations sufficient to eliminate all *rad52Δ* and *rad52Δ srs2Δ* cells (Fig. 2A and Ref. [78]). Taken together, these data indicate that physiological SUMOylation of Rad52 and Rad59 has no pronounced impact on survival after DNA damage. In haploids, the SUMO-mimetic *RAD52-SMT3ΔGG* allele causes *SRS2*-dependent sensitivity to Zeocin but not to MMS (Fig. 2A, upper panel; compare *RAD52-SMT3ΔGG* with *srs2Δ RAD52-SMT3ΔGG; and RAD52-SMT3ΔGG RAD59-SMT3ΔGG* with *srs2*Δ *RAD52-SMT3ΔGG RAD59-SMT3ΔGG*). In *srs2*Δ diploids, the *RAD52-SMT3ΔGG* allele promotes survival on Zeocin and the combination of *RAD52-SMT3ΔGG* with *RAD59-SMT3ΔGG* additionally promotes survival on MMS. Notably, the Rad52-SMT3ΔGG and Rad59-SMT3ΔGG protein levels are slightly higher than wild type after Zeocin treatment (Fig. 2B and C), which may contribute to the increased survival. Taken together, the non-physiological fusion of SUMO to Rad52 and Rad59 caused Zeocin sensitivity in the *SRS2* background but rescued the survival of *srs2*Δ diploid cells, pointing to a primary role for SUMO regulation of Rad52 in DNA double-strand break repair, while fusion of SUMO to both Rad52 and Rad59 were required to rescue the MMS sensitivity of *srs2*Δ cell, indicating redundant roles for SUMOylation of Rad52 and Rad59 during the response to replication stress.

3.4. SUMOylation of Rad52 and Rad59 affects intra- and interchromosomal recombination

To determine the impact of Rad52 and Rad59 SUMOylation on the outcome of recombination, we measured spontaneous direct-repeat recombination (DRR) in haploid cells and interchromosomal heteroallelic recombination in diploids [79] (Fig. 3A). To investigate whether Srs2 impacts HR in the *rad52* and *rad59* mutant strains, recombination rates were measured in both *SRS2* and *srs2*Δ backgrounds. In agreement with previous reports [80,81], *srs2*Δ cells exhibit elevated spontaneous recombination rates in both assays (Fig. 3B and C). In the absence of Rad52 and Rad59 SUMOylation in the *SRS2* haploid

background, the *rad52-3KR*, the *rad59-2KR* and the *rad52-3KR rad59-2KR* double mutant strains all exhibit elevated rates of DRR of which the latter was statistically significant. Likewise, *srs2*Δ *rad52-3KR* and *srs2*Δ *rad59-2KR* double mutant and the *srs2*Δ *rad52-3KR rad59-2KR* triple mutant strains exhibited elevated rates of DRR compared to the *srs2*Δ single mutant. In this case the effects are statistically significant for the two double mutant strains. Next, we investigated the effect of the SUMO-mimetic *rad52-SMT3ΔGG* and *rad59-SMT3ΔGG* mutants in the assays. In the presence of Srs2, we observed increased rates of DRR in strains harbouring these mutations. Notably, the increased rates are mostly due to Rad51-independent SSA events. Interestingly, when the *rad52-SMT3ΔGG* allele was paired with the *srs2*Δ allele, it suppressed the hyper-recombination rate induced by the absence of Srs2. Together these results point to a role of SUMOylation in controlling the outcome of recombination.

Next, we examined the effect of the SUMO mutations in interchromosomal heteroallelic recombination. In diploid *SRS2* cells, both the *rad59-2KR, rad59-SMT3ΔGG*, and *rad52-SMT3ΔGG* alleles showed reduced rates. Similarly, when Srs2 is absent, the double mutants *rad52-3KR rad59-2KR, rad52-3KR rad59-SMT3ΔGG*, and *rad52-SMT3ΔGG rad59-SMT3ΔGG* reduced interchromosomal recombination. The fact that we observe reduced recombination rates in Rad52 and Rad59 mutants that cannot be SUMOylated as well for mutants that are “constitutively” SUMOylated, collectively points to a role of both SUMOylation and deSUMOylation of Rad52 and Rad59 in facilitating interhomolog recombination.

Since exposure to MMS induces both HR and SUMOylation of Rad52-Rad59, we measured MMS-induced direct-repeat and heteroallelic recombination in mutants of *RAD52* and *RAD59* that either abolish SUMOylation or mimic constitutive SUMOylation (Supplementary Fig. S3). As expected, MMS treatment increased the frequency of recombinants by 15–20 fold in the wild type (data not shown), but surprisingly the MMS-induced recombination was largely unaffected by the SUMOylation status of Rad52-Rad59. An exception is the *rad52-SMT3ΔGG* allele, which reduced GC in the direct-repeat recombination assay by three fold, and the *rad52-3KR* allele, which increased heteroallelic recombination by two fold. These differences from spontaneous recombination suggest that the recombination machinery respond differently to the types of DNA lesions that trigger spontaneous recombination than to those induced by MMS. A). Because Rad59 forms a complex with Rad52 [18].

To gain further insight into the impact of SUMOylation on different types of recombination, we also investigated its effects on break-induced replication (BIR) and inverted-repeat recombination (Fig. 4). In the BIR assay [75], the non-SUMOylatable *rad52-3KR* and *rad59-2KR* mutants exhibited a small decrease in recombination, while in the inverted-repeat recombination assay [9], an increase in the recombination rate was observed (Fig. 4).

Overall, the ability to both SUMOylate and deSUMOylate Rad52 and Rad59 seems to act as a positive dynamic regulator for genetically silent recombination between sister chromatids as well as a facilitator of efficient interhomolog recombination, thereby suppressing genetic rearrangements and other potentially genotoxic non-conservative recombination events.

3.5. Rad59 interacts with the Rad52 self-association domain

In vitro, Rad52 forms oligomeric rings by self-association through the N-terminal DNA binding domain [8,82], which also shares homology with Rad59 [9]. To reach a mechanistic understanding of the SUMO-mediated regulation of HR in context of the Rad52-Rad59 complex, we next sought to identify the Rad59 interaction domain within Rad52. To this end, we performed yeast two-hybrid analysis of a collection of Rad52 N-terminal domain mutants [70] against Rad59, Rad51 or Rad52 itself. For each pairwise two-hybrid interaction, the activity of the β-galactosidase reporter was quantified in Miller units and normalized to the wild-type control [69] (Supplementary Fig. S4A–C). This analysis identified *rad52* mutations Y80F, W84A, R85A, Y96A, F110A, R127A, K159A, and F173A that compromise its self-association. Similarly, this analysis identified four *rad52* point mutations (F110A, R127A, K159A and F173A) that disrupt the interaction of Rad52 with Rad59, while not significantly affecting its interaction with Rad51 (Supplementary Fig. S4A). To confirm this observation, we generated fluorescently tagged *rad52-F110A-CFP RAD59-YFP* strain, since the *rad52-F110A* mutation most dramatically reduced the interaction with Rad59. We found that mutating Rad52 residue F110 to alanine abolished any detectable recruitment of Rad59 into the nucleus without changing the total amount of Rad59 in the cell (Fig. 5 A and B), which is similar to the effect obtained by a full deletion of *RAD52* [83]. Taken together, these analyses further confirm that Rad59 interacts with Rad52 at residue F110 in the Rad52 self-association domain.

3.6. Rad59 SUMOylation stabilizes its interaction with Rad52 *in vivo*

We next tested the potential impact of SUMOylation on the Rad52-Rad59 interaction in the yeast two-hybrid assay. To ensure that the endogenous Rad52 and Rad59 would not interfere with the interaction between the GAD and GBD fused forms, the assay was performed in a *rad52*Δ *rad59*Δ strain. This analysis showed that the *rad52-3KR* and *rad59-2KR* mutations did not significantly affect the Rad52-Rad59 interaction, while the interaction was abolished by the *rad52-F110A* mutation (Fig. 5C). Similar conclusion was reached when we tested the effect of Rad59 SUMOylation on its interaction with Rad52 *in vitro* (Supplementary Fig. S2E). Taken together, these results suggest that the interaction between Rad52 and Rad59 is unaffected by SUMOylation.

Since mutation of the SUMO-acceptor lysines in Rad52 and Rad59 did not significantly affect their interaction in the yeast two-hybrid analysis, we decided to test the Rad52-Rad59 interaction in a more physiological setup using bimolecular fluorescence complementation (BiFC) after induction of DNA damage by treatment with Zeocin [84] (Fig. 5D). To this end, *RAD59* variants (*RAD59, rad59-3KR, rad59-SMT3ΔGG*) were fused to a sequence encoding the N-terminal fragment of the fluorescent Venus protein (VN) and *RAD52* variants (*RAD52, rad52-3KR, rad52-F110A, rad52-SMT3ΔGG*) were fused with a sequence encoding the C-terminal complementary fragment (VC). Reconstitution of the Venus fluorescence signal by BiFC allowed us to visualize and quantify *in vivo* the strength of the interaction by quantification of the fluorescence signal generated by pairwise combinations of VN- and VC-tagged proteins (Fig. 5E and F). Mutants carrying the *rad52-3KR* allele had a BiFC signal comparable to wild-type *RAD52*, while the *rad52-F110A* allele showed a reduction in the nuclear fluorescence signal obtained with all forms of *RAD59* (Fig. 5E and

F). Interestingly, the Rad59-Smt3ΔGG fusion showed increased interaction with Rad52 and Rad52-3KR. Moreover, Rad52-Smt3ΔGG showed increased interaction with both Rad59 and Rad59-2KR. Thus, the BiFC analysis indicates that SUMOylation of Rad52 and Rad59 promotes their interaction.

3.7. Rad52 interacts with the E2 conjugating enzyme Ubc9 and with Smt3

To explore Rad52 covalent and non-covalent interaction with SUMO, we analyzed the interaction of wild-type Rad52 and non-SUMOylatable Rad52-3KR with the E2 conjugating enzyme Ubc9, full-length Smt3 and the non-conjugatable variant Smt3ΔGG by yeast two-hybrid. Both Rad52 variants were able to interact with Ubc9. As expected, SUMOylation-deficient Rad52-3KR showed a decrease in interaction with SUMO, while not significantly reducing its ability to interact with Ubc9 (Fig. 5G).

3.8. SUMOylation of Rad52 and Rad59 regulates Srs2 and Rad51 foci formation

Sparked by the *SRS2*-dependent variations in recombination rates in *rad59-SMT3ΔGG*, we hypothesized that the SUMOylated Rad52-Rad59 complex participates in recruiting Srs2 to sites of DNA damage. To test this hypothesis we determined the amount of Srs2 present at Rad52 foci after DSB induction with Zeocin (Fig. 6A–C). This analysis revealed a significant reduction in Srs2 recruitment in cells engineered to mimic constitutive SUMOylation of Rad52 or Rad59, while only the *rad52-3KR rad59-2KR* mutant reduced Rad52 recruitment to foci compared to the wild type (Fig. 6B and C). Since Srs2 has the capability to displace Rad51 from ssDNA [22–26], we analyzed Rad51 foci after Zeocin treatment of wild type, SUMO-deficient *rad52-3KR rad59-2KR* and SUMO-mimetic *rad52-SMT3ΔGG rad59-SMT3ΔGG* double mutants. These combinations were analyzed in both *SRS2* and *srs2Δ* backgrounds. As expected, the intensity of Rad51 foci was higher in all *srs2Δ* strains (Fig. 6D and E). Importantly, in the *SRS2* background, the intensity of Rad51 foci formed in *rad52-3KR rad59-2KR* mutant strains was significantly higher than those formed in the wild-type background. Conversely, *rad52-SMT3ΔGG rad59-SMT3ΔGG* cells showed an Srs2-dependent decrease in Rad51 focus intensity (Fig. 6D and E). To test if the changes in Srs2 and Rad51 recruitment to foci affect their loading onto DNA at a DSB, we examined the binding of Srs2 and Rad51 to an HO-induced DSB at the mating-type locus using chromatin immunoprecipitation (Supplementary Fig. S5). This analysis did not reveal any significant dependency on Rad52-Rad59 SUMOylation for loading of Srs2 or Rad51 onto DNA at the *HO* cut-site on Rad52-Rad59 SUMOylation, indicating that recruitment to foci and DNA binding are controlled separately for these proteins.

4. Discussion

Rad52 and Rad59 are known to physically interact [18]. Here we have demonstrated that this interaction is enhanced *in vivo* when the two proteins are SUMOylated (Fig. 5E). However, the interaction does not strictly depend on SUMOylation, as non-SUMOylatable mutants of Rad52 and Rad59 still interact. Because the Rad59 binding domain in Rad52 overlaps with the Rad52 self-association domain (Supplementary Fig. S4), we propose that Rad59 could be incorporated into Rad52 rings in a manner [15,16], where SUMOylation regulates the equilibrium between Rad52 rings that do or do not contain Rad59 (Fig. 7). Incorporation of

Rad59 into Rad52 rings could reduce the ability of the ring to recruit Rad51, because Rad59 does not interact with Rad51 [15], or because SUMO may directly obstruct interaction with Rad51. To test this hypothesis, we examined the role of Rad52 and Rad59 SUMOylation in recruitment of Rad51 to DNA lesions. Consistent with our hypothesis, the quantitative analysis of Rad51 foci revealed less intense Rad51 foci when Rad52 and Rad59 are "constitutively" SUMOylated. Inversely, we observed a greater intensity of Rad51 foci, when Rad52 and Rad59 cannot be SUMOylated. We note, however, that within the sensitivity of chromatin immunoprecipitation, SUMOylation of Rad52-Rad59 does not appear to quantitatively affect the loading of Rad51 onto DNA at a DSB (Supplementary Fig. S5).

Analysis of direct-repeat recombination in haploid cells showed an increased ratio of Leu^+Ura^+ (gene conversion) to Leu^+Ura^- (single-strand annealing) recombinants in non-SUMOylatable mutants and the opposite in mutants that mimic constitutive SUMOylation (Fig. 3B), suggesting that SUMOylation of Rad52 and Rad59 stimulate recombination outcomes based on annealing rather than pathways that require Rad51-catalyzed strand invasion. Similar, although less pronounced effects are observed in the absence of Srs2, suggesting that this effect is largely independent of Srs2. In diploid cells, we observed a reduction in interhomolog recombination for both non-SUMOylatable and SUMO-mimetic mutants (Fig. 3C), which could reflect a general decrease in recombination efficiency or increased preference for intrachromosomal recombination. The latter is supported by the general increase in direct-repeat recombination for both non-SUMOylatable and SUMO-mimetic mutants (Fig. 3B). This suggests that both SUMO conjugation and deconjugation are necessary for the full biological function of this post-translational modification and that the dynamics of (de)SUMOylation is required to achieve rearrangement-free, genetically silent recombinational repair possibly through SUMO-dependent remodeling of DNA-protein intermediates. Further, the effects of Rad59 SUMOylation may be related to the ability of Rad59 to promote sister chromatid cohesion through its interaction with RSC (remodel structure of chromatin) complex [85], hence, counteracting inter-chromosome based repair.

The observed increase in inverted-repeat recombination in the non-SUMOylatable *rad52-3KR rad59-2KR* mutant provides additional evidence that SUMOylation of the Rad52-Rad59 complex promotes rearrangement-free recombination with the sister chromatid or intra-molecularly. In contrast, BIR was decreased in the *rad52-3KR* and in the *rad52-3KR rad59-2KR* mutants. Since several successive invasion events are thought to be required to complete BIR [86], our data indicates that efficient strand invasion is promoted by SUMOylation of Rad52. Alternatively, the small reduction in BIR in the *rad52-3KR* and in the *rad52-3KR rad59-2KR* mutants may reflect the lower steady-state level of the non-SUMOylatable variants of these proteins (Fig. 2B and C and [44]). Controlling Rad52 and Rad59 activity through SUMOylation could be particularly important to suppress non-conservative modes of recombinational repair at repetitive sequences, which may otherwise lead to translocations and telomere–telomere recombination [2,87–90].

Rad59 SUMOylation does not dramatically impact cell survival after DNA damage, similarly to Rad52 SUMOylation [50]. Interestingly, in diploid cells, the Rad52-Smt3ΔGG

fusion rescued the Zeocin sensitivity of *srs2*Δ cells and Rad52-Smt3ΔGG together with Rad59-Smt3ΔGG rescued the MMS sensitivity. Since MMS treatment leads to replication stress and most known suppressors of *srs2*Δ reduce Rad51 nucleoprotein filament formation [78,91,92], we propose that SUMOylation of Rad59 is important for restraining toxic Rad51-mediated recombination during replication stress. This conclusion goes well with other reports of a role for Rad59 in DNA replication stress tolerance [3,93,94]. Similarly, the fact that we observed reduced recombination and increased MMS and Zeocin survival of *srs2*Δ cells when mimicking constitutive SUMOylation of Rad52 is in agreement with the recent finding that toxic Rad51-dependent HR structures fail to form in *srs2Δ rad52-SMT3ΔGG* [78] and with the reduced recruitment of Rad51 to foci in the *rad52-SMT3ΔGG rad59-SMT3ΔGG* mutant (Fig. 6D). Alternatively, the suppression of Zeocin sensitivity of the *srs2*Δ mutant by *rad52-SMT3ΔGG rad59-SMT3ΔGG* may reflect the increased Rad52 and Rad59 protein levels of the SUMO mimetic variants (Fig. 2B and C). Taken together, our findings suggest that Rad59, instead of exclusively engaging in SSA, plays a secondary yet important role together with Rad52 in controlling Rad51-dependent recombination events as it has been previously suggested [95].

The physical interaction between the Rad59 and Rad52 paralogues in their N-terminal domains [15,16] and co-localization *in vivo* [83] indicate that the two proteins act in a heteromeric complex. This is further supported by biochemical studies demonstrating that both proteins can catalyze annealing of complementary DNA strands [7, 18–21, 96] and genetic studies placing the two genes in the same epistasis group [9, 97]. It is therefore tempting to speculate that SUMOylation of Rad52 and Rad59 may play similar roles during recombination *in vivo*. Indeed, we observed synergy between SUMOylation of the two proteins in several assays. First, the SUMO-mimetic fusions of Rad52 and Rad59 synergistically rescued the MMS sensitivity of the *srs2*Δ diploid strain (Fig. 2A). Second, the non-SUMOylatable *rad52-3KR* and *rad59-2KR* mutants synergistically increased spontaneous direct-repeat recombination in *SRS2* cells (Fig. 3B) and decreased interhomolog recombination in *srs2*Δ cells (Fig. 3C). Third, the non-SUMOylatable *rad52-3KR* and *rad59-2KR* mutants synergistically increased spontaneous inverted-repeat recombination in *rad51Δ* cells (Fig. 4D). These synergistic effects are consistent with redundancy between the SUMOylation sites on Rad52 and Rad59.

It has become clear that SUMOylation represents a widespread response to DNA damage, targeting a number of proteins involved in recombinational repair, from the initial factors that recognize the DNA lesion and checkpoint proteins that halt the cell cycle for repair, down to the last steps of recombination [42, 43]. With this study we provide functional insight into the promotion of conservative HR by SUMOylation of the Rad52-Rad59 complex.

Supplementary Material

Refer to Web version on PubMed Central for supplementary material.

Acknowledgments

We thank members of the Lisby, Regenberg and Holmberg laboratories for helpful discussions on this work, Hoa Phan for technical assistance, and Hannah Klein, Jim Haber, Lorraine Symington, Dana Branzei, Rodney Rothstein, Yoshiko Kikuchi and Stefan Åström for sharing reagents. This work was supported by The Danish Agency for Science, Technology and Innovation, the Villum Kann Rasmussen Foundation, the Lundbeck Foundation, the European Research Council (ERC) to M.L. and I.G., Fundação para a Ciência e Tecnologia (FCT) to S.S., Czech Science Foundation (GACR 13-26629S and 207/12/2323), and European Regional Development Fund (Project FNUSA-ICRC) (No. CZ.1.05/1.1.00/02.0123) grants to L.K., "Employment of Newly Graduated Doctors of Science for Scientific Excellence" (CZ.1.07/2.3.00/30.0009) co-financed from European Social Fund and funds from the Faculty of Medicine, Masaryk University, to V.A., and NIH grant GM080670, American Cancer Society grant RSG-12-013-01-CCG, and Leukemia and Lymphoma Society Scholar Award to X.Z.

Appendix A. Supplementary data

Supplementary data associated with this article can be found, in the online version, at http://dx.doi.org/10.1016/j.dnarep.2016.04.001.

References

1. Symington LS, Rothstein R, Lisby M. Mechanisms and regulation of mitotic recombination in *Saccharomyces cerevisiae*. Genetics. 2014; 198:795–835. [PubMed: 25381364]
2. Mott C, Symington LS. RAD51-independent inverted-repeat recombination by a strand-annealing mechanism. DNA Repair (Amst). 2011; 10:408–415. [PubMed: 21317047]
3. Nguyen HD, Becker J, Thu YM, Costanzo M, Koch EN, Smith S, Myung K, Myers CL, Boone C, Bielinsky AK. Unligated Okazaki fragments induce PCNA ubiquitination and a requirement for Rad59-dependent replication fork progression. PLoS One. 2013; 8:e66379. [PubMed: 23824283]
4. Ozenberger BA, Roeder GS. A unique pathway of double-strand break repair operates in tandemly repeated genes. Mol Cell Biol. 1991; 11:1222–1231. [PubMed: 1996088]
5. Sugawara N, Haber JE. Characterization of double-strand break-induced recombination: homology requirements and single-stranded DNA formation. Mol Cell Biol. 1992; 12:563–575. [PubMed: 1732731]
6. Ivanov EL, Sugawara N, Fishman-Lobell J, Haber JE. Genetic requirements for the single-strand annealing pathway of double-strand break repair in *Saccharomyces cerevisiae*. Genetics. 1996; 142:693–704. [PubMed: 8849880]
7. Mortensen UH, Bendixen C, Sunjevaric I, Rothstein R. DNA strand annealing is promoted by the yeast Rad52 protein. Proc Natl Acad Sci U S A. 1996; 93:10729–10734. [PubMed: 8855248]
8. Shinohara A, Shinohara M, Ohta T, Matsuda S, Ogawa T. Rad52 forms ring structures and co-operates with RPA in single-strand DNA annealing. Genes Cells. 1998; 3:145–156. [PubMed: 9619627]
9. Bai Y, Symington LS. A Rad52 homolog is required for *RAD51*-independent mitotic recombination in *Saccharomyces cerevisiae*. Genes Dev. 1996; 10:2025–2037. [PubMed: 8769646]
10. Signon L, Malkova A, Naylor ML, Klein H, Haber JE. Genetic requirements for RAD51- and RAD54-independent break-induced replication repair of a chromosomal double-strand break. Mol Cell Biol. 2001; 21:2048–2056. [PubMed: 11238940]
11. Chen Q, Ijpma A, Greider CW. Two survivor pathways that allow growth in the absence of telomerase are generated by distinct telomere recombination events. Mol Cell Biol. 2001; 21:1819–1827. [PubMed: 11238918]
12. Krejci L, Song B, Bussen W, Rothstein R, Mortensen UH, Sung P. Interaction with Rad51 is indispensable for recombination mediator function of Rad52. J Biol Chem. 2002; 277:40132–40141. [PubMed: 12171935]
13. Krejci L, Altmannova V, Spirek M, Zhao X. Homologous recombination and its regulation. Nucleic Acids Res. 2012; 40:5795–5818. [PubMed: 22467216]
14. Sung P, Krejci L, Van Komen S, Sehorn MG. Rad51 recombinase and recombination mediators. J Biol Chem. 2003; 278:42729–42732. [PubMed: 12912992]

15. Davis AP, Symington LS. The Rad52-Rad59 complex interacts with Rad51 and replication protein A. DNA Repair (Amst). 2003; 2:1127–1134. [PubMed: 13679150]
16. Cortes-Ledesma F, Malagon F, Aguilera A. A novel yeast mutation *rad52-L89F*, causes a specific defect in Rad51-independent recombination that correlates with a reduced ability of Rad52-L89F to interact with Rad59. Genetics. 2004; 168:553–557. [PubMed: 15454565]
17. Feng Q, During L, de Mayolo AA, Lettier G, Lisby M, Erdeniz N, Mortensen UH, Rothstein R. Rad52 and Rad59 exhibit both overlapping and distinct functions. DNA Repair (Amst). 2007; 6:27–37. [PubMed: 16987715]
18. Davis AP, Symington LS. The yeast recombinational repair protein Rad59 interacts with Rad52 and stimulates single-strand annealing. Genetics. 2001; 159:515–525. [PubMed: 11606529]
19. Petukhova G, Stratton SA, Sung P. Single strand DNA binding and annealing activities in the yeast recombination factor Rad59. J Biol Chem. 1999; 274:33839–33842. [PubMed: 10567339]
20. Wu Y, Kantake N, Sugiyama T, Kowalczykowski SC. Rad51 protein controls Rad52-mediated DNA annealing. J Biol Chem. 2008; 283:14883–14892. [PubMed: 18337252]
21. Wu Y, Sugiyama T, Kowalczykowski SC. DNA annealing mediated by Rad52 and Rad59 proteins. J Biol Chem. 2006; 281:15441–15449. [PubMed: 16565518]
22. Colavito S, Macris-Kiss M, Seong C, Gleeson O, Greene EC, Klein HL, Krejci L, Sung P. Functional significance of the Rad51-Srs2 complex in Rad51 presynaptic filament disruption. Nucleic Acids Res. 2009; 37:6754–6764. [PubMed: 19745052]
23. Krejci L, Macris M, Li Y, Van Komen S, Villemain J, Ellenberger T, Klein H, Sung P. Role of ATP hydrolysis in the antirecombinase function of *Saccharomyces cerevisiae* Srs2 protein. J Biol Chem. 2004; 279:23193–23199. [PubMed: 15047689]
24. Krejci L, Van Komen S, Li Y, Villemain J, Reddy MS, Klein H, Ellenberger T, Sung P. DNA helicase Srs2 disrupts the Rad51 presynaptic filament. Nature (Lond). 2003; 423:305–309. [PubMed: 12748644]
25. Qiu Y, Antony E, Doganay S, Koh HR, Lohman TM, Myong S. Srs2 prevents Rad51 filament formation by repetitive motion on DNA. Nat Commun. 2013; 4:2281. [PubMed: 23939144]
26. Veaute X, Jeusset J, Soustelle C, Kowalczykowski SC, Le Cam E, Fabre F. The Srs2 helicase prevents recombination by disrupting Rad51 nucleoprotein filaments. Nature (Lond). 2003; 423:309–312. [PubMed: 12748645]
27. Burgess RC, Lisby M, Altmannova V, Krejci L, Sung P, Rothstein R. Localization of recombination proteins and Srs2 reveals anti-recombinase function in vivo. J Cell Biol. 2009; 185:969–981. [PubMed: 19506039]
28. Chanet R, Heude M, Adjiri A, Maloisel L, Fabre F. Semidominant mutations in the yeast Rad51 protein and their relationships with the Srs2 helicase. Mol Cell Biol. 1996; 16:4782–4789. [PubMed: 8756636]
29. Palladino F, Klein HL. Analysis of mitotic and meiotic defects in *Saccharomyces cerevisiae* SRS2 DNA helicase mutants. Genetics. 1992; 132:23–37. [PubMed: 1327956]
30. Vaze MB, Pellicioli A, Lee SE, Ira G, Liberi G, Arbel-Eden A, Foiani M, Haber JE. Recovery from checkpoint-mediated arrest after repair of a double-strand break requires Srs2 helicase. Mol Cell. 2002; 10:373–385. [PubMed: 12191482]
31. Yeung M, Durocher D. Srs2 enables checkpoint recovery by promoting disassembly of DNA damage foci from chromatin. DNA Repair (Amst). 2011; 10:1213–1222. [PubMed: 21982442]
32. Prakash S, Prakash L, Burke W, Monteleone B. Effects of the *RAD52* gene on recombination in *Saccharomyces cerevisiae*. Genetics. 1980; 94:31–50. [PubMed: 17248995]
33. Lee PS, Petes TD. From the cover: mitotic gene conversion events induced in G1-synchronized yeast cells by gamma rays are similar to spontaneous conversion events. Proc Natl Acad Sci U S A. 2010; 107:7383–7388. [PubMed: 20231456]
34. Fabre F, Chan A, Heyer WD, Gangloff S. Alternate pathways involving Sgs1/Top3, Mus81/Mms4, and Srs2 prevent formation of toxic recombination intermediates from single-stranded gaps created by DNA replication. Proc Natl Acad Sci U S A. 2002; 99:16887–16892. [PubMed: 12475932]
35. Lettier G, Feng Q, de Mayolo AA, Erdeniz N, Reid RJ, Lisby M, Mortensen UH, Rothstein R. The role of DNA double-strand breaks in spontaneous homologous recombination in *S. cerevisiae*. PLoS Genet. 2006; 2:1773–1786.

36. Mozlin AM, Fung CW, Symington LS. Role of the *Saccharomyces cerevisiae* Rad51 paralogs in sister chromatid recombination. Genetics. 2008; 178:113–126. [PubMed: 18202362]
37. Jackson SP, Durocher D. Regulation of DNA damage responses by ubiquitin and SUMO. Mol Cell. 2013; 49:795–807. [PubMed: 23416108]
38. van Wijk SJ, Muller S, Dikic I. Shared and unique properties of ubiquitin and SUMO interaction networks in DNA repair. Genes Dev. 2011; 25:1763–1769. [PubMed: 21896653]
39. Nagai S, Davoodi N, Gasser SM. Nuclear organization in genome stability: SUMO connections. Cell Res. 2011; 21:474–485. [PubMed: 21321608]
40. Bergink S, Jentsch S. Principles of ubiquitin and SUMO modifications in DNA repair. Nature (Lond). 2009; 458:461–467. [PubMed: 19325626]
41. Altmannova V, Kolesar P, Krejci L. SUMO wrestles with recombination. Biomolecules. 2012; 2:350–375. [PubMed: 24970142]
42. Cremona CA, Sarangi P, Yang Y, Hang LE, Rahman S, Zhao X. Extensive DNA damage-induced sumoylation contributes to replication and repair and acts in addition to the mec1 checkpoint. Mol Cell. 2012; 45:422–432. [PubMed: 22285753]
43. Psakhye I, Jentsch S. Protein group modification and synergy in the SUMO pathway as exemplified in DNA repair. Cell. 2012; 151:807–820. [PubMed: 23122649]
44. Sacher M, Pfander B, Hoege C, Jentsch S. Control of Rad52 recombination activity by double-strand break-induced SUMO modification. Nat Cell Biol. 2006; 8:1284–1290. [PubMed: 17013376]
45. Burgess RC, Rahman S, Lisby M, Rothstein R, Zhao X. The Slx5-Slx8 complex affects sumoylation of DNA repair proteins and negatively regulates recombination. Mol Cell Biol. 2007; 27:6153–6162. [PubMed: 17591698]
46. Kolesar P, Sarangi P, Altmannova V, Zhao X, Krejci L. Dual roles of the SUMO-interacting motif in the regulation of Srs2 sumoylation. Nucleic Acids Res. 2012; 40:7831–7843. [PubMed: 22705796]
47. Saponaro M, Callahan D, Zheng X, Krejci L, Haber JE, Klein HL, Liberi G. Cdk1 targets Srs2 to complete synthesis-dependent strand annealing and to promote recombinational repair. PLoS Genet. 2010; 6:e1000858. [PubMed: 20195513]
48. Adzuma K, Ogawa T, Ogawa H. Primary structure of the *RAD52* gene in *Saccharomyces cerevisiae*. Mol Cell Biol. 1984; 4:2735–2744. [PubMed: 6098821]
49. Antúnez de Mayolo A, Lisby M, Erdeniz N, Thybo T, Mortensen UH, Rothstein R. Multiple start codons and phosphorylation result in discrete Rad52 protein species. Nucl Acids Res. 2006; 34:2587–2597. [PubMed: 16707661]
50. Altmannova V, Eckert-Boulet N, Arneric M, Kolesar P, Chaloupkova R, Damborsky J, Sung P, Zhao X, Lisby M, Krejci L. Rad52 SUMOylation affects the efficiency of the DNA repair. Nucleic Acids Res. 2010; 38:4708–4721. [PubMed: 20371517]
51. Torres-Rosell J, Sunjevaric I, De Piccoli G, Sacher M, Eckert-Boulet N, Reid R, Jentsch S, Rothstein R, Aragon L, Lisby M. The Smc5-Smc6 complex and SUMO modification of Rad52 regulates recombinational repair at the ribosomal gene locus. Nat Cell Biol. 2007; 9:923–931. [PubMed: 17643116]
52. Bergink S, Ammon T, Kern M, Schermelleh L, Leonhardt H, Jentsch S. Role of Cdc48/p97 as a SUMO-targeted segregase curbing Rad51-Rad52 interaction. Nat Cell Biol. 2013; 15:526–532. [PubMed: 23624404]
53. Armstrong AA, Mohideen F, Lima CD. Recognition of SUMO-modified PCNA requires tandem receptor motifs in Srs2. Nature (Lond). 2012; 483:59–63. [PubMed: 22382979]
54. Kim SO, Yoon H, Park SO, Lee M, Shin JS, Ryu KS, Lee JO, Seo YS, Jung HS, Choi BS. Srs2 possesses a non-canonical PIP box in front of its SBM for precise recognition of SUMOylated PCNA. J Mol Cell Biol. 2012; 4:258–261. [PubMed: 22641647]
55. Sherman, F.; Fink, GR.; Hicks, JB. Methods in Yeast Genetics. Cold Spring Harbor Laboratory; Cold Spring Harbor, N Y: 1986.
56. Erdeniz N, Mortensen UH, Rothstein R. Cloning-free PCR-based allele replacement methods. Genome Res. 1997; 7:1174–1183. [PubMed: 9414323]

57. Silva S, Gallina I, Eckert-Boulet N, Lisby M. Live cell microscopy of DNA damage response in *Saccharomyces cerevisiae*. Methods Mol Biol. 2012; 920:433–443. [PubMed: 22941621]
58. Heim R, Tsien RY. Engineering green fluorescent protein for improved brightness, longer wavelengths and fluorescence resonance energy transfer. Curr Biol. 1996; 6:178–182. [PubMed: 8673464]
59. Ormo M, Cubitt AB, Kallio K, Gross LA, Tsien RY, Remington SJ. Crystal structure of the *Aequorea victoria* green fluorescent protein [see comments]. Science. 1996; 273:1392–1395. [PubMed: 8703075]
60. Keppler-Ross S, Noffz C, Dean N. A new purple fluorescent color marker for genetic studies in *Saccharomyces cerevisiae* and *Candida albicans*. Genetics. 2008; 179:705–710. [PubMed: 18493083]
61. Zhao X, Blobel G. A SUMO ligase is part of a nuclear multiprotein complex that affects DNA repair and chromosomal organization. Proc Natl Acad Sci U S A. 2005; 102:4777–4782. [PubMed: 15738391]
62. Seong C, Colavito S, Kwon Y, Sung P, Krejci L. Regulation of Rad51 recombinase presynaptic filament assembly via interactions with the Rad52 mediator and the Srs2 anti-recombinase. J Biol Chem. 2009; 284:24363–24371. [PubMed: 19605344]
63. Seong C, Sehorn MG, Plate I, Shi I, Song B, Chi P, Mortensen U, Sung P, Krejci L. Molecular anatomy of the recombination mediator function of *Saccharomyces cerevisiae* Rad52. J Biol Chem. 2008; 283:12166–12174. [PubMed: 18310075]
64. Shi I, Hallwyl SC, Seong C, Mortensen U, Rothstein R, Sung P. Role of the Rad52 amino-terminal DNA binding activity in DNA strand capture in homologous recombination. J Biol Chem. 2009; 284:33275–33284. [PubMed: 19812039]
65. Hays SL, Firmenich AA, Massey P, Banerjee R, Berg P. Studies of the interaction between Rad52 protein and the yeast single-stranded DNA binding protein RPA. Mol Cell Biol. 1998; 18:4400–4406. [PubMed: 9632824]
66. Plate I, Hallwyl SC, Shi I, Krejci L, Muller C, Albertsen L, Sung P, Mortensen UH. Interaction with RPA is necessary for Rad52 repair center formation and for its mediator activity. J Biol Chem. 2008; 283:29077–29085. [PubMed: 18703507]
67. Kawabe Y, Seki M, Seki T, Wang WS, Imamura O, Furuichi Y, Saitoh H, Enomoto T. Covalent modification of the Werner's syndrome gene product with the ubiquitin-related protein, SUMO-1. J Biol Chem. 2000; 275:20963–20966. [PubMed: 10806190]
68. James P, Halladay J, Craig EA. Genomic libraries and a host strain designed for highly efficient two-hybrid selection in yeast. Genetics. 1996; 144:1425–1436. [PubMed: 8978031]
69. Miller, JH. Formulas and Recipes. Cold Spring Harbor Laboratory; New York: 1972.
70. Mortensen UH, Erdeniz N, Feng Q, Rothstein R. A molecular genetic dissection of the evolutionarily conserved N terminus of yeast Rad52. Genetics. 2002; 161:549–562. [PubMed: 12072453]
71. Hoekstra MF, Naughton T, Malone RE. Properties of spontaneous mitotic recombination occurring in the presence of the *rad52-1* mutation of *Saccharomyces cerevisiae*. Genet Res. 1986; 48:9–17. [PubMed: 3536661]
72. Smith J, Rothstein R. An allele of RFA1 suppresses RAD52-dependent double-strand break repair in *Saccharomyces cerevisiae*. Genetics. 1999; 151:447–458. [PubMed: 9927442]
73. Rosche WA, Foster PL. Determining mutation rates in bacterial populations. Methods (San Diego Calif). 2000; 20:4–17.
74. Hall BM, Ma CX, Liang P, Singh KK. Fluctuation analysis CalculatOR: a web tool for the determination of mutation rate using Luria–Delbruck fluctuation analysis. Bioinformatics (Oxf Engl). 2009; 25:1564–1565.
75. Davis AP, Symington LS. RAD51-dependent break-induced replication in yeast. Mol Cell Biol. 2004; 24:2344–2351. [PubMed: 14993274]
76. Johnson ES, Schwienhorst I, Dohmen RJ, Blobel G. The ubiquitin-like protein Smt3p is activated for conjugation to other proteins by an Aos1p/Uba2p heterodimer. EMBO J. 1997; 16:5509–5519. [PubMed: 9312010]

77. Le Breton C, Dupaigne P, Robert T, Le Cam E, Gangloff S, Fabre F, Veaute X. Srs2 removes deadly recombination intermediates independently of its interaction with SUMO-modified PCNA. Nucleic Acids Res. 2008; 36:4964–4974. [PubMed: 18658248]

78. Esta A, Ma E, Dupaigne P, Maloisel L, Guerois R, Le Cam E, Veaute X, Coic E. Rad52 sumoylation prevents the toxicity of unproductive Rad51 filaments independently of the anti-recombinase Srs2. PLoS Genet. 2013; 9:e1003833. [PubMed: 24130504]

79. Smith J, Rothstein R. A mutation in the gene encoding the *Saccharomyces cerevisiae* single-stranded DNA-binding protein Rfa1 stimulates a RAD52-independent pathway for direct-repeat recombination. Mol Cell Biol. 1995; 15:1632–1641. [PubMed: 7862154]

80. Pfander B, Moldovan GL, Sacher M, Hoege C, Jentsch S. SUMO-modified PCNA recruits Srs2 to prevent recombination during S phase. Nature (Lond). 2005; 436:428–433. [PubMed: 15931174]

81. Rong L, Palladino F, Aguilera A, Klein HL. The hyper-gene conversion hpr5-1 mutation of *Saccharomyces cerevisiae* is an allele of the SRS2/RADH gene. Genetics. 1991; 127:75–85. [PubMed: 1849857]

82. Van Dyck E, Hajibagheri NM, Stasiak A, West SC. Visualisation of human rad52 protein and its complexes with hRad51 and DNA. J Mol Biol. 1998; 284:1027–1038. [PubMed: 9837724]

83. Lisby M, Barlow JH, Burgess RC, Rothstein R. Choreography of the DNA damage response; spatiotemporal relationships among checkpoint and repair proteins. Cell. 2004; 118:699–713. [PubMed: 15369670]

84. Sung MK, Huh WK. Bimolecular fluorescence complementation analysis system for in vivo detection of protein–protein interaction in *Saccharomyces cerevisiae*. Yeast. 2007; 24:767–775. [PubMed: 17534848]

85. Oum JH, Seong C, Kwon Y, Ji JH, Sid A, Ramakrishnan S, Ira G, Malkova A, Sung P, Lee SE, Shim EY. RSC facilitates Rad59-dependent homologous recombination between sister chromatids by promoting cohesin loading at DNA double-strand breaks. Mol Cell Biol. 2011; 31:3924–3937. [PubMed: 21807899]

86. Smith CE, Llorente B, Symington LS. Template switching during break-induced replication. Nature (Lond). 2007; 447:102–105. [PubMed: 17410126]

87. Churikov D, Charifi F, Simon MN, Geli V. Rad59-facilitated acquisition of Y′ elements by short telomeres delays the onset of senescence. PLoS Genet. 2014; 10:e1004736. [PubMed: 25375789]

88. Doerfler L, Harris L, Viebranz E, Schmidt KH. Differential genetic interactions between Sgs1 DNA-damage checkpoint components and DNA repair factors in the maintenance of chromosome stability. Genome Integr. 2011; 2:8. [PubMed: 22040455]

89. Pannunzio NR, Manthey GM, Bailis AM. RAD59 and RAD1 cooperate in translocation formation by single-strand annealing in *Saccharomyces cerevisiae*. Curr Genet. 2010; 56:87–100. [PubMed: 20012294]

90. Ruiz JF, Gomez-Gonzalez B, Aguilera A. Chromosomal translocations caused by either pol32-dependent or pol32-independent triparental break-induced replication. Mol Cell Biol. 2009; 29:5441–5454. [PubMed: 19651902]

91. Liu J, Renault L, Veaute X, Fabre F, Stahlberg H, Heyer WD. Rad51 paralogues Rad55-Rad57 balance the antirecombinase Srs2 in Rad51 filament formation. Nature (Lond). 2011; 479:245–248. [PubMed: 22020281]

92. Aboussekhra A, Chanet R, Adjiri A, Fabre F. Semidominant suppressors of Srs2 helicase mutations of *Saccharomyces cerevisiae* map in the *RAD51* gene, whose sequence predicts a protein with similarities to procaryotic RecA proteins. Mol Cell Biol. 1992; 12:3224–3234. [PubMed: 1620127]

93. Lee M, Lee CH, Demin AA, Munashingha PR, Amangyeld T, Kwon B, Formosa T, Seo YS. Rad52/Rad59-dependent recombination as a means to rectify faulty Okazaki fragment processing. J Biol Chem. 2014; 289:15064–15079. [PubMed: 24711454]

94. Liddell LC, Manthey GM, Owens SN, Fu BX, Bailis AM. Alleles of the homologous recombination gene RAD59, identify multiple responses to disrupted DNA replication in *Saccharomyces cerevisiae*. BMC Microbiol. 2013; 13:229. [PubMed: 24125552]

95. Wu D, Topper LM, Wilson TE. Recruitment and dissociation of nonhomologous end joining proteins at a DNA double-strand break in *Saccharomyces cerevisiae*. Genetics. 2008; 178:1237–1249. [PubMed: 18245831]

96. Nimonkar AV, Sica RA, Kowalczykowski SC. Rad52 promotes second-end DNA capture in double-stranded break repair to form complement-stabilized joint molecules. Proc Natl Acad Sci U S A. 2009; 106:3077–3082. [PubMed: 19204284]

97. Jablonovich Z, Liefshitz B, Steinlauf R, Kupiec M. Characterization of the role played by the RAD59 gene of *Saccharomyces cerevisiae* in ectopic recombination. Curr Genet. 1999; 36:13–20. [PubMed: 10447590]

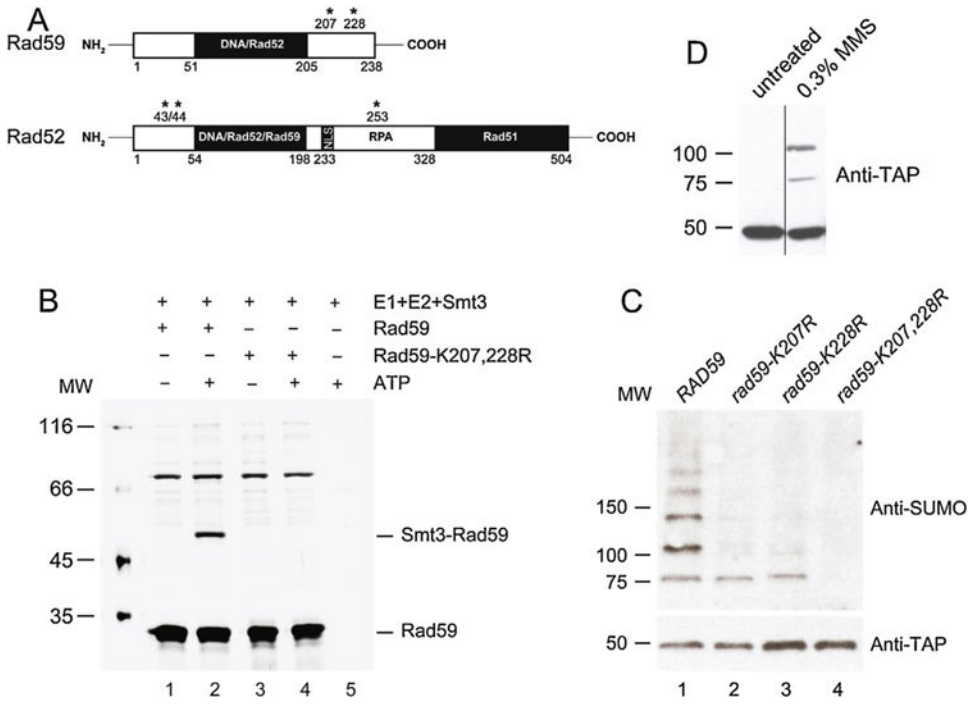

Fig. 1.

The lysine residues 207 and 228 of Rad59 are required for its SUMOylation. (A) Domain organization of Rad59 and Rad52. The position of SUMOylated lysines is marked with asterisks. Nuclear localization signal (NLS), and DNA/protein interaction domains are indicated. (B) *In vitro* SUMOylation of Rad59. *In vitro* SUMOylation assays were performed with recombinant Aos1/Uba2 (400 nM), Ubc9 (2.8 μM) and Smt3 (5.6 μM) in the presence or absence of ATP, and with either wild type or SUMO-deficient Rad59 mutant (5.6 μM). The reaction mixtures were incubated for 1 h at 4 °C and stopped by adding 10 μl of SDS-Laemmli PAGE. The samples were analyzed on 10% SDS-PAGE followed by silver staining. (C) *In vivo* SUMOylation of Rad59. In each of the indicated strains (X3078-6C, G514, G515, and G516), Rad59-TAP was tandem affinity purified, followed by protein transfer and detection with anti-SUMO and anti-TAP antibodies. Cells were treated with 0.3% MMS for 2 h. (D) Mobility shift of Rad59 upon DNA damage. Rad59 was tagged with a tandem affinity purification (TAP) tag. Total cell extract was examined after protein transfer with anti-TAP antibody. Cells (X4692-1B) were untreated or treated with 0.3% MMS for 2 h.

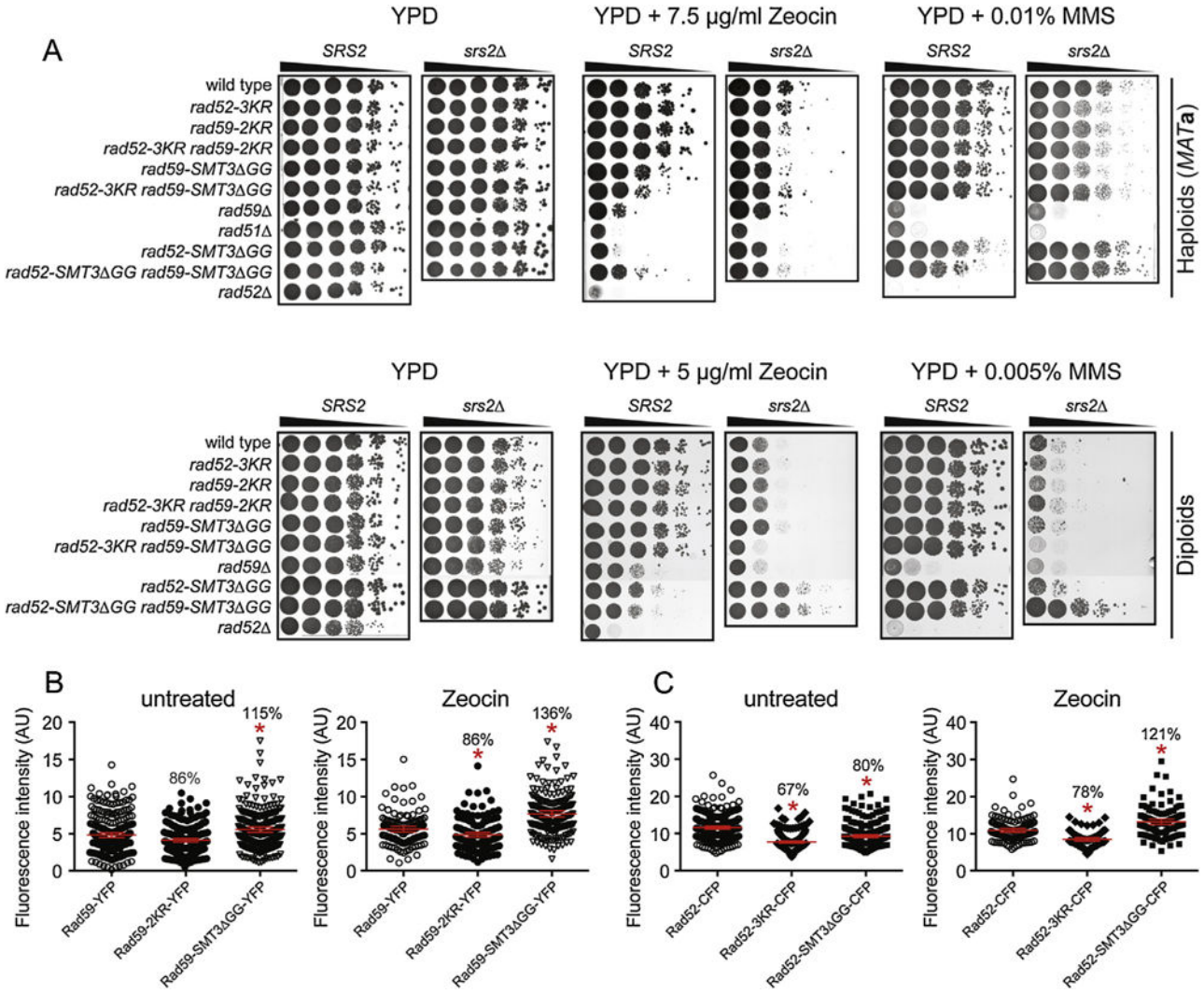

Fig. 2.

SUMOylation mimetic *rad52-SMT3ΔGG* and *rad59-SMT3ΔGG* alleles suppress the DNA damage sensitivity of *srs2*Δ diploid cells. (A) Impact of SUMOylation on cell survival following genotoxic stress. Ten-fold serial dilutions of the haploid strains (ML144-8C, ML458-7B, ML392-2A, ML461-1B, SS44-5D, SS47-20A, ML459-5B, SS6-29D, SS56-19C, SS56-27B, ML390-3D, SS52-4D, SS3-8B, SS3-8D, SS256-2B, SS47-21A, SS47-19B, SS35-10A, SS8-8D, SS130-10B, and SS202-4B) and the diploid strains (ML412, ML480, ML415, ML463, ML611, ML613, ML413, ML787, ML785 ML414, ML478, ML591, ML599, ML600, ML612, ML614, ML577, ML788, ML786, and ML414) were spotted onto YPD or YPD containing the indicated concentrations of Zeocin or MMS and incubated for 3 days at 30 °C before acquiring images. Representative composite images are shown that were obtained using the same batch of media. A *rad52Δ srs2Δ* double mutant was omitted because it is known to be exquisitely sensitive to DNA damage [78]. Genotypes of strains are listed in Supplementary Table S1. (B and C) Protein levels of SUMOylation defective and mimetic mutants. Rad52 and Rad59 protein abundances were determined by measuring the whole nuclear fluorescence signal of the CFP-tagged Rad52 and YFP-tagged

Rad59 protein variants before and after treatment with 300 μg/ml Zeocin for 2 h in wild-type (NEB110-25B), *rad52-3KR* (NEB111-5D), *rad59-2KR* (ML640-2D), *rad59-SMT3ΔGG* (SS116-57B) and *rad52-SMT3ΔGG* (SS199-1B) cells. Each data point represents one cell measurement. Error bars represent 95% confidence intervals in red. Statistically significant differences ($p < 0.05$) were determined using nonparametric Dunn's multiple comparisons test. Significant differences from the wild type are marked with a red asterisk (*) and the mean protein level relative to the wild type is indicated. AU, arbitrary units. (B) Rad59-YFP fluorescence levels. (C) Rad52-CFP fluorescence levels.

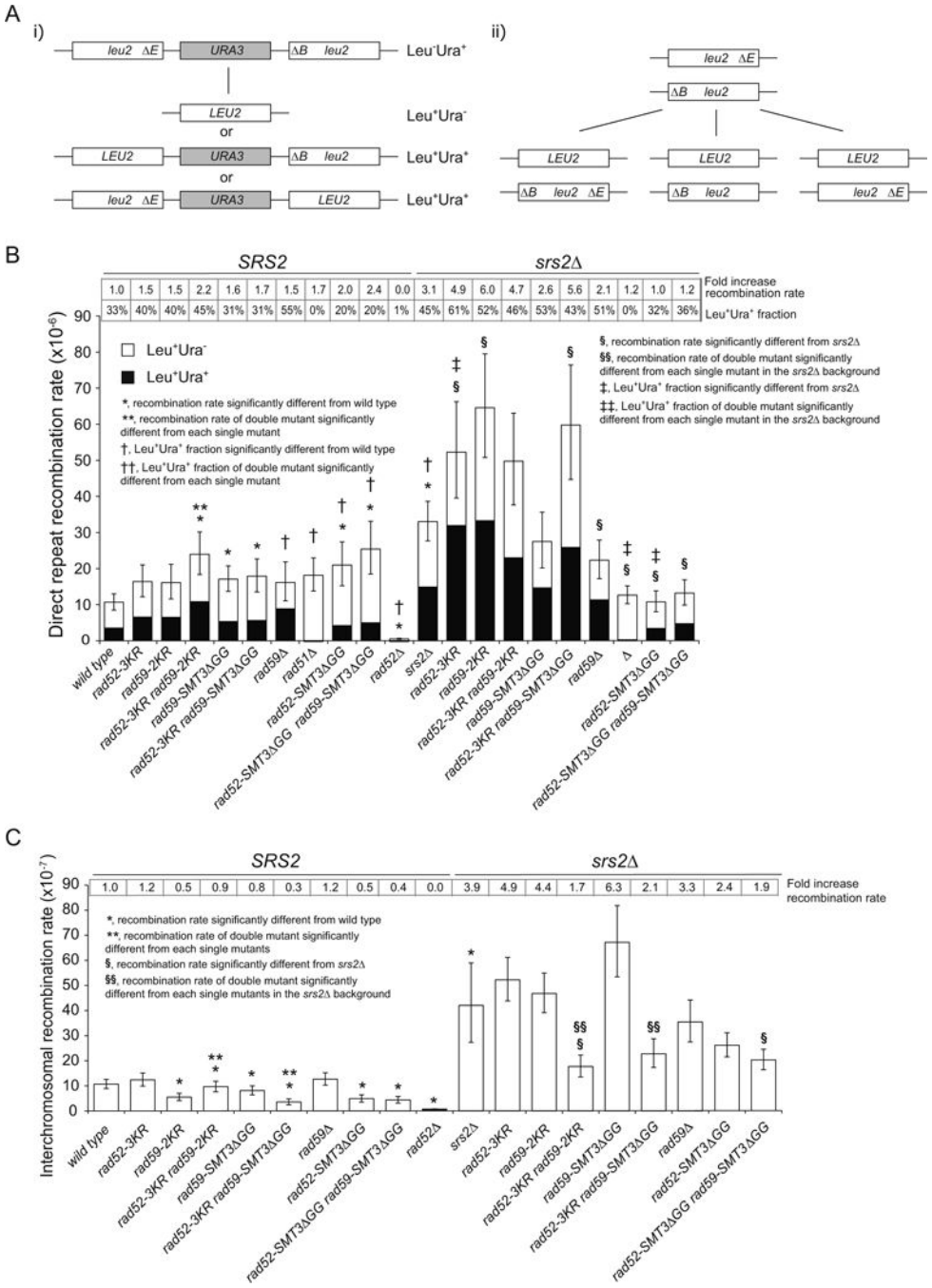

Fig. 3.

SUMOylation of Rad52 and Rad59 promotes rearrangement-free mitotic recombination. (A) Schematic representation of the assays used for measuring direct-repeat (i) and heteroallelic (ii) recombination between *leu2-ΔEcoRI* and *leu2-ΔBstEII* heteroalleles. (B) Mitotic recombination between direct repeats in haploid cells (ML144-8C, ML458-7B, ML392-2A, ML461-1B, SS44-5D, SS47-20A, ML459-5B, SS6-29D, SS56-1B, SS56-27B, ML390-3D, SS52-4D, SS3-8B, SS3-8D, SS256-2B, SS47-21A, SS47-19B, SS35-10A, SS8-8D, SS130-10B, and SS202-4B). The fold increase relative to wild type recombination rate is

indicated above each bar. For each bar, the fraction shaded in black corresponds to gene conversion (GC, Leu^+Ura^+) events and is indicated above each bar as percentage of total events. The white fraction of each bar corresponds to the single-strand annealing (SSA, Leu^+Ura^-) fraction. For each genotype, ≥702 Leu^+ colonies in 9–19 independent cultures were tested for uracil prototrophy. (C) Mitotic heteroallelic recombination in diploid cells (ML412, ML480, ML415, ML463, ML611, ML613, ML413, ML787, ML785, ML414, ML478, ML591, ML599, ML600, ML612, ML614, ML577, ML788, and ML786). All recombination rates are presented as events per cell per generation. For each strain, 9–19 trials were performed. Error bars correspond to the 95% confidence interval as calculated by the FALCOR MSS Maximum Likelihood algorithm [73,74]. Changes in recombination rates and GC ratios were compared using unpaired T-test and considered significant if $P < 0.05$. Genotypes of strains are listed in Supplementary Table S1.

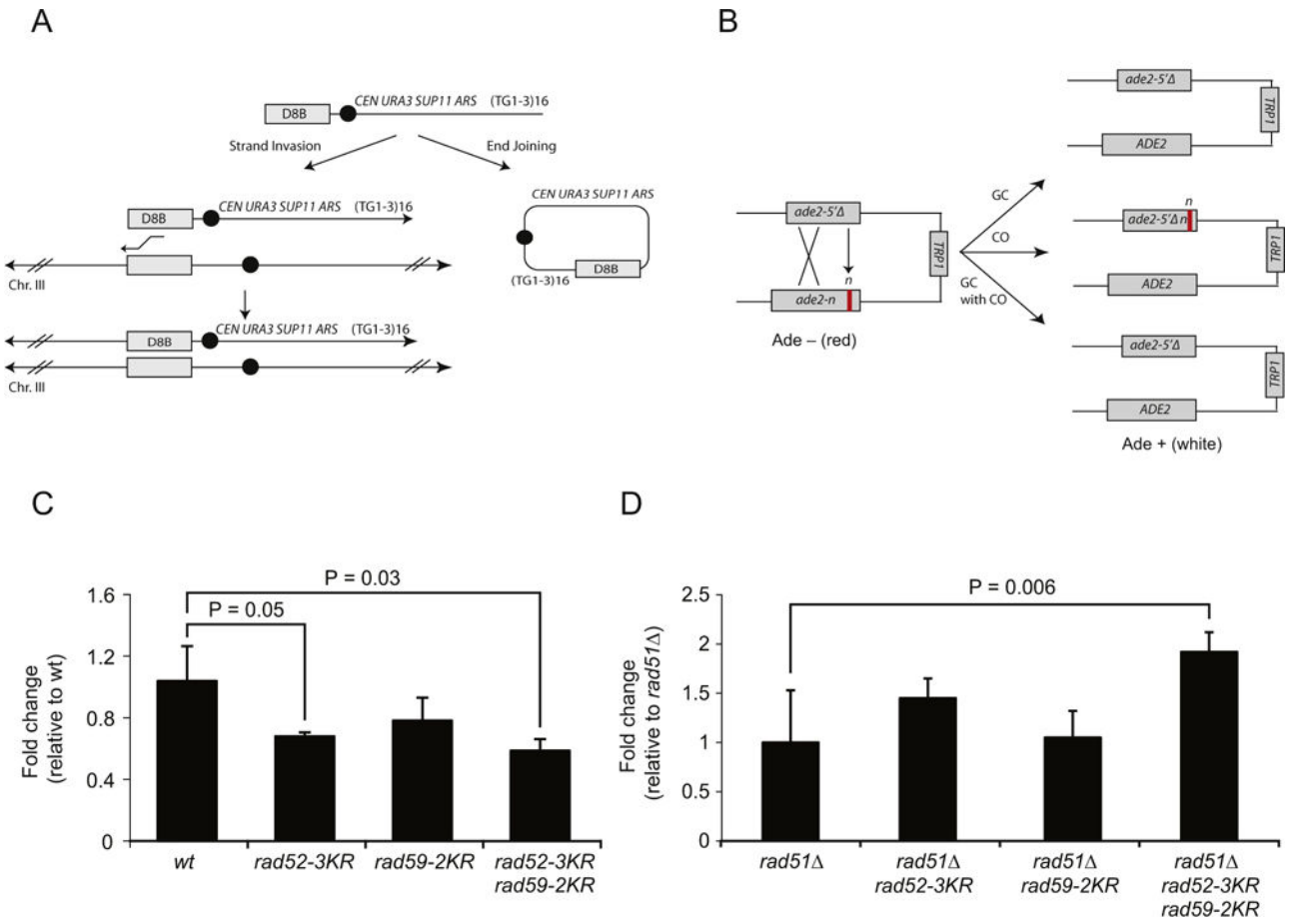

Fig. 4.

The *rad52-3KR* and *rad59-2KR* mutants exhibit reduced BIR and increased inverted-repeat recombination. (A) Assay for BIR. The schematic illustrates the BIR assay [75]. (B) Assay for inverted-repeat recombination. The schematic illustrates the *ade2* inverted-repeat recombination assay [9]. (C) Sumoylation of Rad52 promotes BIR. Strains (W1588-4C, X1974-1B, X1974-1C, and X1974-1D) were assayed for BIR as described in Section 2. (D) Sumoylation of Rad52 and Rad59 suppresses inverted-repeat recombination. Strains (X2002-46B, X2004-5A, X2142-10A, and X2142-5A) were assayed for inverted-repeat recombination as described in Section 2.

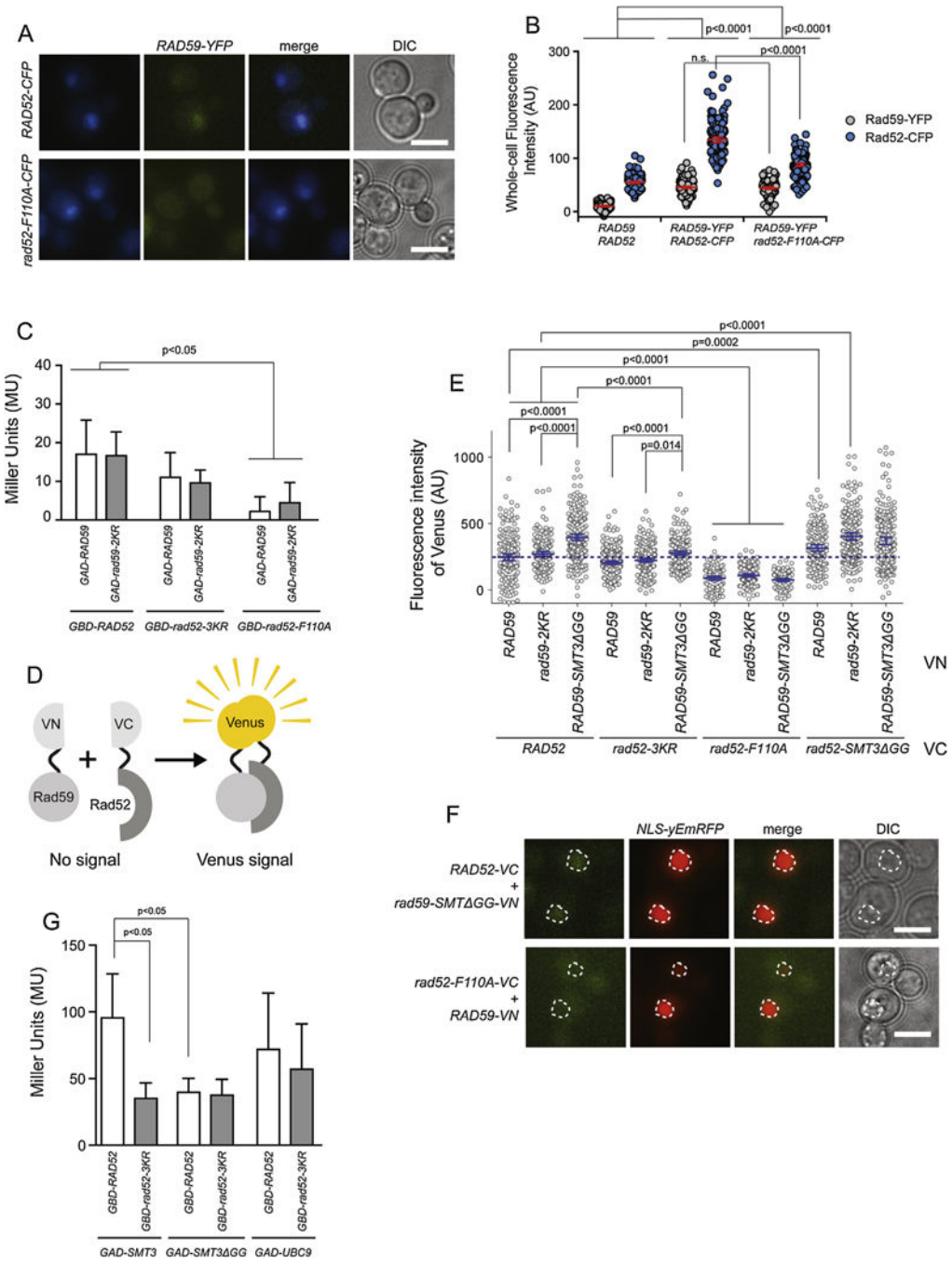

Fig. 5.

SUMOylation and distinct residues on Rad52 regulate its interaction with Rad59. (A) Nuclear localization of Rad59 is abolished in the *rad52-F110A* mutant. Cells expressing either wild type Rad52-CFP (NEB110-25B) or Rad52-F110A-CFP (SS163-15A) were used to investigate Rad59-YFP localization by fluorescence microscopy. (B) Quantification of whole-cell fluorescence. The Rad59-YFP and Rad52-CFP mean fluorescence intensities were quantified for the experiment in panel (A). A strain with untagged Rad52 and Rad59 was used as a negative control (ML8-9A). Each point represents the mean fluorescence

intensity of one cell. Bars and whiskers represent the mean value and 95% confidence intervals, respectively. (C) Association of Rad52 with Rad59. Reporter strains W2274-9B (*MAT***a**) were transformed with GAD-fused Rad59 variants and W2274-1C (*MATα*) were transformed with GBD-fused *RAD52* variants and the interactions between the two proteins were analyzed in diploids after mating. Error bars represent SD and statistical significance was calculated using unpaired T-test for multiple comparisons. (C,G) β-galactosidase activities of the two-hybrid assay correspond to the background-corrected Miller units ($MU_{corrected}$), where the background was defined as the signal generated by each of the pGAD and pGBD carrying the different fusion proteins against the pGAD and pGBD empty vectors ($MU_{corrected} = MU_{XxY} - MU_{GADxY} - MU_{XxGBD} + MU_{GADxGBD}$). (D) Schematic illustration of bimolecular fluorescence complementation (BiFC) assay. To analyze the Rad52-Rad59 interaction by BiFC, strains carry pairwise combinations of Rad52 and Rad59 variants tagged with non-fluorescent C- (VC) and N-terminal (VN) fragments of Venus, respectively. (E–F) Rad52 residue F110 and SUMO promotes its association with Rad59. Strains (SS169-19B, SS171-1B, SS177-4D, SS170-2A, SS172-2A, SS176-15B, SS188-3C, SS180-1B, SS187-2B, SS183-22C, SS181-1C, and SS179-31A) were transformed with a plasmid expressing mRFP-NLS as a nuclear marker and grown in SC-Leu medium to OD_{600} = 0.2. Prior to microscopy, all cell cultures were treated for 2 h with 300 μg/ml of Zeocin, harvested and prepared for image acquisition. (E) Whole-nuclear fluorescence quantification of the Rad52-Rad59 interaction. Each point represents the BiFC intensity of one nucleus. Bars and whiskers represent the mean value and 95% confidence intervals, respectively. Dashed line indicates the level of fluorescence generated by wild-type Rad52-VC and Rad59-VN. (F) Representative images in the upper panel show a BiFC signal within the nucleus, indicating a direct association between Rad52-VC and Rad59-Smt3ΔGG-VN. Representative images in the lower panel show the lack of a BiFC signal, evidencing an impaired association between Rad52-F110A-VC and Rad59-VN. A white dashed line highlights the nuclear area. Genotypes of strains are listed in Supplementary Table S1. Scale bar 3 μm. (G) Association of Rad52 with SUMO and Ubc9. GAD-fused to full-length Smt3, Smt3ΔGG and the SUMO E2-conjugating enzyme Ubc9, were tested for association with the two variants of Rad52 fused to GBD by yeast two-hybrid. Error bars represent standard deviation (SD) and statistical significance ($p < 0.05$) was calculated using unpaired T-test for multiple comparisons.

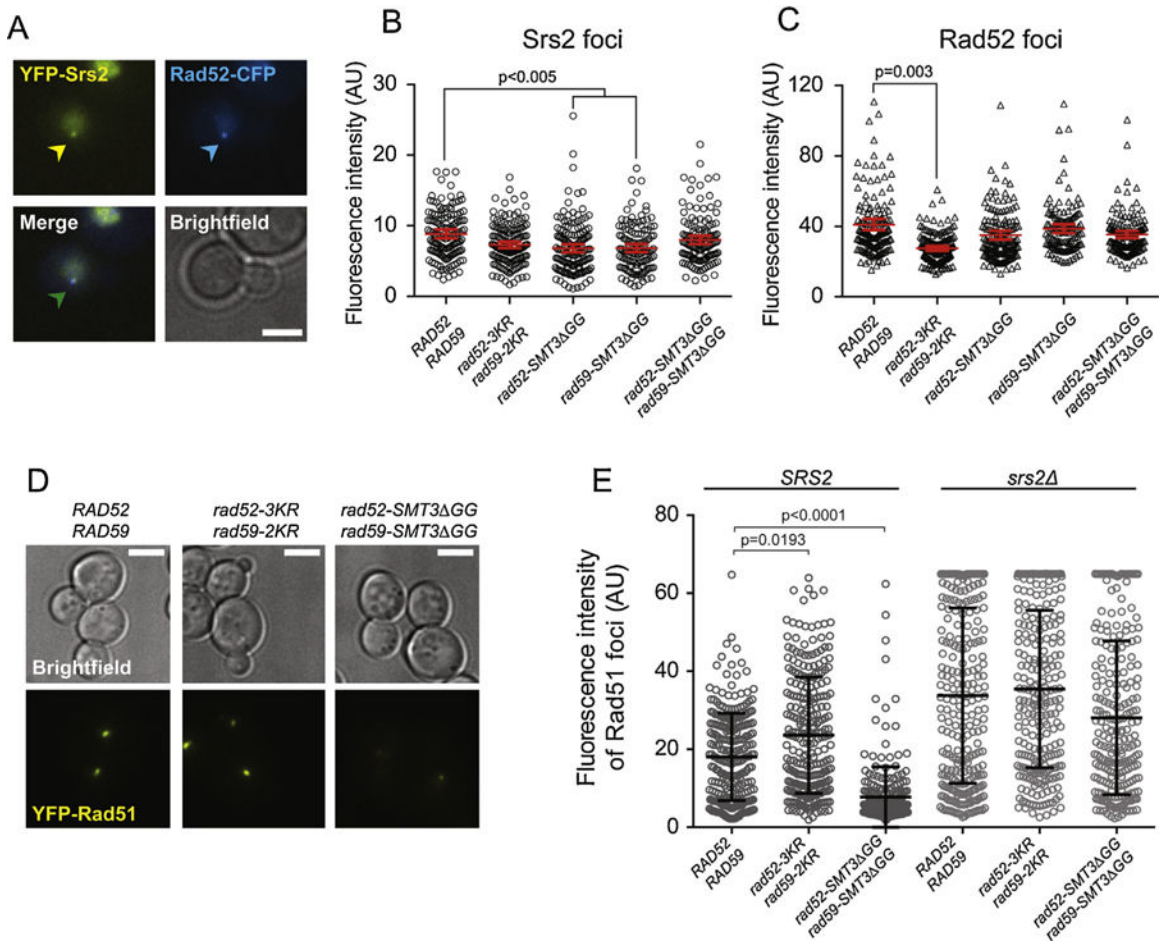

Fig. 6.

SUMOylation status of the Rad52-Rad59 complex regulates Srs2 and Rad51 recruitment to foci. (A–C) Cells expressing YFP-Srs2 and Rad52-CFP in wild type (NEB280-5B), *rad52-3KR rad59-2KR* (SS276-4B), *rad52-SMT3ΔGG* (SS275-1A), *rad59-SMT3ΔGG* (SS278-10C) and *rad52-SMT3ΔGG rad59-SMT3ΔGG* (SS279-7B) backgrounds were treated with 250 μg/ml Zeocin for 1 h prior to imaging. (A) Representative image for YFP-Srs2 focus colocalizing with Rad52-CFP. (B) Distribution of fluorescence signal intensities for YFP-Srs2 measured at Rad52-CFP foci. (D–E) Strains expressing YFP-Rad51 and different variants of *RAD52 RAD59* in both *SRS2* and *srs2Δ* backgrounds (SS239-2C, wild type; SS244-5D, *srs2Δ*; SS242-34D, *rad52-SMT3ΔGG rad59-SMT3ΔGG*; SS249-1C, *rad52-SMT3ΔGG rad59-SMT3ΔGG srs2Δ*; SS250-1A, *rad52-3KR rad59-2KR*; SS255-1C, *rad52-3KR rad59-2KR srs2Δ*) were grown in SC + Ade medium at 25 °C to OD_{600} = 0.2 and treated with 300 μg/ml of Zeocin prior to imaging. (D) Representative images for Rad51 foci. (E) Distribution of fluorescence signal intensities for Rad51 foci. Each point represents the intensity of one focus. Bars represent the mean value and standard deviation for each strain. Scale bars 3 μm.

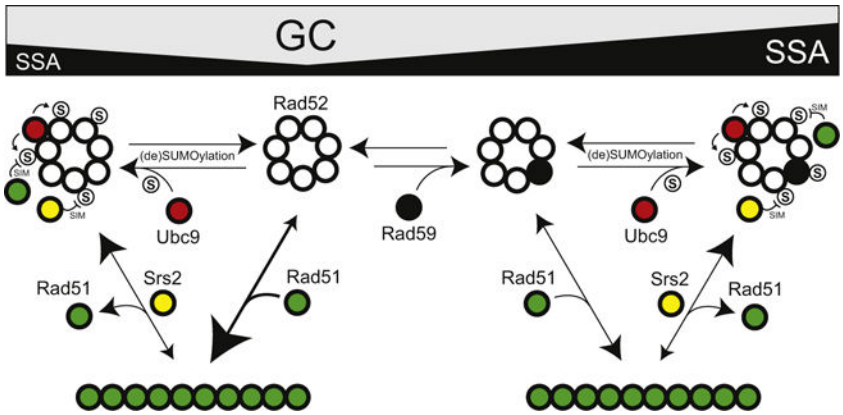

Fig. 7.

Model for regulation of HR by Rad59 and Rad52 SUMOylation. Rad52 rings exist in a dynamic equilibrium with or without Rad59, which promotes repair by single-strand annealing (SSA). DNA damage stimulates SUMOylation of both Rad52 and Rad59, which could stabilize the Rad52-Rad59 complex to shift the balance in favor of SSA at the expense of gene conversion (GC) between sister-chromatids or intra-molecularly. The interaction of Rad52 with the Ubc9 SUMO conjugating enzyme may promote SUMOylation of the Rad52-Rad59 complex. The recruitment of the Rad51 recombinase and the Srs2 anti-recombinase to SUMOylated Rad52-Rad59 via the SIMs in Rad51 [52] and Srs2 [46] may serve to continuously remodel recombination complexes to promote disassembly of non-productive Rad51 filaments.